

THERMAL COMFORT USING RANQUE-HILSCH VORTEX TUBE

A DISSERTATION

*Submitted in partial fulfillment of the
requirements for the award of the degree*

of

MASTER OF TECHNOLOGY

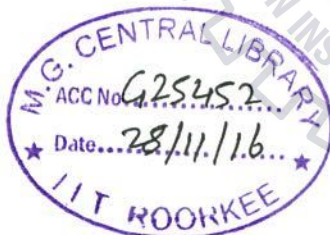
in

MECHANICAL ENGINEERING

(With Specialization in Thermal Engineering)

By

VIVEKANAND



**DEPARTMENT OF MECHANICAL AND INDUSTRIAL ENGINEERING
INDIAN INSTITUTE OF TECHNOLOGY ROORKEE
ROORKEE - 247 667 (INDIA)
MAY, 2016**



INDIAN INSTITUTE OF TECHNOLOGY ROORKEE

CANDIDATE'S DECLARATION

I hereby declare that the work carried out in this dissertation entitled “**THERMAL COMFORT USING RANQUE–HILSCH VORTEX TUBE**”, is presented in partial fulfillment of the requirements for the award of degree of “**Master of Technology**” in **Mechanical Engineering** with specialization in **Thermal Engineering** submitted to the Department of **Mechanical and Industrial Engineering, Indian Institute of Technology, Roorkee, India**, under the supervision and guidance of **Dr. Sudhakar Subudhi**, Associate Professor, Department of Mechanical and Industrial Engineering. I have not submitted the record embodied in this report for the award of any other degree or diploma.

Date: May, 2016

Place: IIT Roorkee

Vivekanand
(VIVEKANAND)

This is to certify that the above statement made by the candidate is correct to the best of my knowledge and belief.

Sudh Subudhi
(Dr. Sudhakar Subudhi) 13-5-2016

Associate Professor
MIED, IIT Roorkee
UK-247 667, India

ACKNOWLEDGEMENTS

I would like to take this opportunity to express my sincere gratitude towards my supervisor **Dr. Sudhakar Subudhi** Associate Professor in the department of **MECHANICAL AND INDUSTRIAL ENGINEERING, INDIAN INSTITUTE OF TECHNOLOGY, ROORKEE**, and my friend Akash Jaiswal without whose support this work would have been impossible. I would like to thank them for their suggestions, motivation and spending their precious time in discussion about topic and continuous guidance.

I express my sincere thanks to the **Indian Institute of Technology Roorkee** for providing with the infrastructure for fulfillment of my project requirement. I am also express my sincere thanks to all faculty members and staff of Mechanical and Industrial Engineering Department.

I extend my thanks to all friends especially Chandan Swaroop Meena, Kanhaiya, Deepak Kumar, Sudhir, Aditya Kumar, Swaroop, Deepak Khurana, Lokesh Tiwari and Rajesh Chaudhary for their help, support, interest and technical conversation about input of my project work.

Finally, this project would not have been possible without the confidence and support of my father Mr. Sita Ram, my mother Mrs. Dhanaoo Devi, my brothers Ravi, Laxmishanker and my sister Krishna. I am very thankful for their unconditional love and support at all stages of my life.

Vivekanand
VIVEKANAND

Enrollment No- 14541019

M.Tech- 2nd Year

Thermal Engineering

ABSTRACT

Thermal comfort is a situation of mind that express satisfaction with ambient condition. It mainly includes following processes: heating, ventilation and cooling. Different parameters that affect the condition of thermal comfort are air temperature, metabolic rate, humidity and wind velocity. In this experimental work we achieved thermal comfort with the help of Ranque- Hilsch vortex tube.

Vortex tube is a self-temperature separating device. It consists of a nozzle, vortex length, orifice and control valve. It can be used as refrigeration machine. Air at high pressure enters the vortex tube and splits in to two parts: one at lower temperature and other one at higher temperature with respect to inlet temperature. We get low temperature due to expansion of air near the inlet nozzle, and high temperature at hot end due to compression of air. Temperature separation is also occurred due to shear between fluid layer, momentum transfer and high swirl speed. But exact explanation for getting temperature separation in vortex tube is still unclear. Vortex tube can be utilized in oil and gas exploration industry, recovering waste energy, low temperature application and predominantly for cooling purposes.

To study the effect of change in thermo-physical properties such as pressure, temperature, mass flow rate on temperature separation, an experimental setup is developed. It is consisting of a pressure regulator, some fittings, and two pressure transducers, two rotameters, two humidity sensors and few T-type of thermocouples.

In this report, the variation of cold and hot temperature drop and humidity at cold exit with different inlet pressures and cold mass fractions.

From experimental result we found cold temperature decreases as cold mass fraction increases up to $\Omega_c \leq 0.5, 0.6$ and then it increases for low pressure. At high pressure cold temperature decreases up to 0.3 ~0.4 and then increases. Hot temperature increases with cold mass fraction as well as with pressure. Relative humidity at exit of cold fluid decreases with the cold mass fraction. But at low pressure, there is very minute changes in humidity. Humidity at high pressure increases at cold side, then decrease as cold mass fraction increases.

COP and cooling efficiency have been calculated for different cold mass fraction and pressure. Cooling efficiency first increase with increase in cold mass fraction and later decreases.

Flow inside vortex tube is turbulent and hence the variation of parameters with the Reynolds number should be instigated. Reynolds number at inlet increases with the pressure. Non-dimensional cold temperature drop increases, and non-dimensional hot temperature drop decreases with the Reynolds number. We have also found that non-dimensional cold temperature drop first increases with the cold mass fraction up to 0.25 to 0.35, later it decreases. Non-dimensional hot temperature drop decrease with the cold mass fraction.



TABLE OF CONTENTS

Chapter No.	Title	Page No.
	ABSTRACT	iv
	TABLE OF CONTENTS	vi
	LIST OF FIGURES	ix
	LIST OF TABLES	xiii
	NOMENCLATURE	xiv
1	INTRODUCTION	1
	1.1 Historical background and progress work on vortex tube	2
	1.2 Vortex tube	4
	1.3 Vortex tube parameter	5
	1.3.1 Cold mass fraction Ω_c	5
	1.3.2 Hot and cold temperature drop	5
	1.3.3 Coefficient of performance	5
	1.3.4 Cooling efficiency	6
	1.3.5 Reynolds number	6
	1.3.6 Non- dimensional temperature drop	7
	1.4 Types of vortex tube	7
	1.4.1 Counter flow vortex tube	7
	1.4.2 Parallel flow vortex tube	8
	1.5 Applications of vortex tube	8
	1.6 Advantages and disadvantages of vortex tube	9
2	LITERATURE REVIEW	10
	2.1 Working principles of Ranque -Hilsch vortex tube	10
	2.2 Mechanism	10
	2.3 Temperature drop in vortex tube	11
	2.4 Vortex tube as classical refrigeration cycle	14
	2.4.1 Heat rejection process (4-1)	15
	2.4.2 Adiabatic expansion (1-3)	15

	2.4.3 Heat absorption process (3-c)	15
	2.4.4 Adiabatic compression process (c-4)	16
	2.5 Study on Ranque- Hilsch vortex tube to increase the moisture removal	16
	2.6 Droplet behavior in Ranque -Hilsch vortex tube	18
	2.7 Geometrical factor affecting the performance of R-H vortex tube	18
	2.7.1 Humidity	19
	2.7.2 Compressed air pressure	19
	2.7.3 Input air temperature	19
3	EXPERIMENTAL METHODOLOGY AND SETUP	20
	3.1 Experimental setup	20
	3.1.1 Air compressor	21
	3.1.2 Pressure regulator	22
	3.1.3 Rotameter	24
	3.1.4 Vortex tube	26
	3.1.5 Humidity sensor	27
	3.1.6 Pressure transducer	28
	3.2 Experimental procedures	29
4	RESULTS AND DISCUSSION	31
	4.1 Variation in hot and cold temperature drops, RH with cold mass fraction	31
	4.2 Analysis of thermo physical properties at Fully open control valve	38
	4.3 Analysis of thermo physical properties at 50% Open control valve	41
	4.4 Analysis of thermo physical properties at Fully close control valve	44
	4.5 Cooling efficiency and Reynolds number analysis on vortex tube	47
	4.6 Reynolds number at different pressure when insulation use on vortex tube	49
	4.7 Reynolds number at different pressure without insulation on vortex tube	51
	4.8 Coefficient of performance of Ranque Hilsch vortex tube	54
5	CONCLUSIONS AND FUTURE SCOPE OF WORK	58

APENDIX	60
1.1 Calculation of cooling capacity for room size(3l x 3bx 3h=27 m ³)	60
1.2 Calibration	61
1.2.1 Pressure transducer	61
1.2.2 Temperature calibration	62
1.2.3 Humidity sensor calibration	63
1.2.4 Rotameter calibration	65
1.2.5 Dynamic viscosity	66
REFERENCES	67



LIST OF FIGURES

Fig. No.	Name of figures	Page No.
1.1	Psychometric chart showing comfort region	1
1.2	Number of publications	3
1.3	Vortex tube counter flow type	5
1.4	Counter flow vortex tube	8
1.5	Parallel flow vortex tube	8
2.1	Secondary circulation	11
2.2	Vortex tube as refrigeration cycle	15
3.1	Photographic view of experimental setup	20
3.2	Reciprocating air compressor	21
3.3	Air pressure regulator	23
3.4	Inside view of air pressure regulator	23
3.5(a)	Air rotameter (CFM) at inlet	25
3.5(b)	Air rotameter (LPM) at cold exit	25
3.6	Vortex tube	26
3.7	Humidity sensor HTG3515CH	27
3.8	Electronic pressure transducer	28
3.9	Line connection of transducer	29
3.10	Schematic diagram of experimental setup	30
4.1	Cold temperature v/s cold mass fraction plot at different inlet pressure without insulation on vortex tube	31
4.2	Cold temperature v/s cold mass fraction plot at different inlet pressure with insulation on vortex tube	32
4.3	Hot temperature v/s cold mass fraction plot at different inlet pressure without insulation on vortex tube	33
4.4	Hot temperature v/s cold mass fraction plot at different inlet pressure with insulation on vortex tube	33
4.5	Cold temperature drop v/s cold mass fraction plot at different inlet pressure without insulation on vortex tube	34

4.6	Cold temperature drop v/s cold mass fraction plot at different inlet pressure with insulation on vortex tube	35
4.7	Hot temperature drop v/s cold mass fraction plot at different inlet pressure without insulation on vortex tube	35
4.8	Hot temperature drop v/s cold mass fraction plot at different inlet pressure with insulation on vortex tube	36
4.9	Variation of relative humidity with cold mass fraction at various input pressure without insulation used on vortex tube	37
4.10	Variation of relative humidity with cold mass fraction at various input pressure when insulation used on vortex tube	38
4.2.1	Variation of cold mass fraction Ω_c with various inlet pressure	38
4.2.2	Variation of cold temperature with various inlet pressure	39
4.2.3	Variation of hot temperature with various inlet pressure	40
4.2.4	Variation of cold and hot temperature drop with various inlet pressure	40
4.2.5	Variation of relative humidity with various inlet pressure	41
4.3.1	Variation of cold mass fraction Ω_c with various inlet pressure	41
4.3.2	Variation of cold temperature with various inlet pressure	42
4.3.3	Variation of hot temperature with various inlet pressure	42
4.3.4	Variation of cold and hot temperature with various inlet pressure	43
4.3.5	Relative humidity with various inlet pressure plot	43
4.4.1	Variation of cold mass fraction Ω_c with various inlet pressure	44
4.4.2	Variation of cold temperature with various inlet pressure	44
4.4.3	Variation of hot temperature with various inlet pressure	45
4.4.4	Variation of cold and hot temperature drop with various inlet pressure	45
4.4.5	Variation of relative humidity with various inlet pressure	46
4.5.1	Variation of cooling efficiency with cold mass fraction at different inlet pressure without insulation on vortex tube	47
4.5.2	Variation of cooling efficiency with cold mass fraction at different inlet pressure with insulation on vortex tube	48

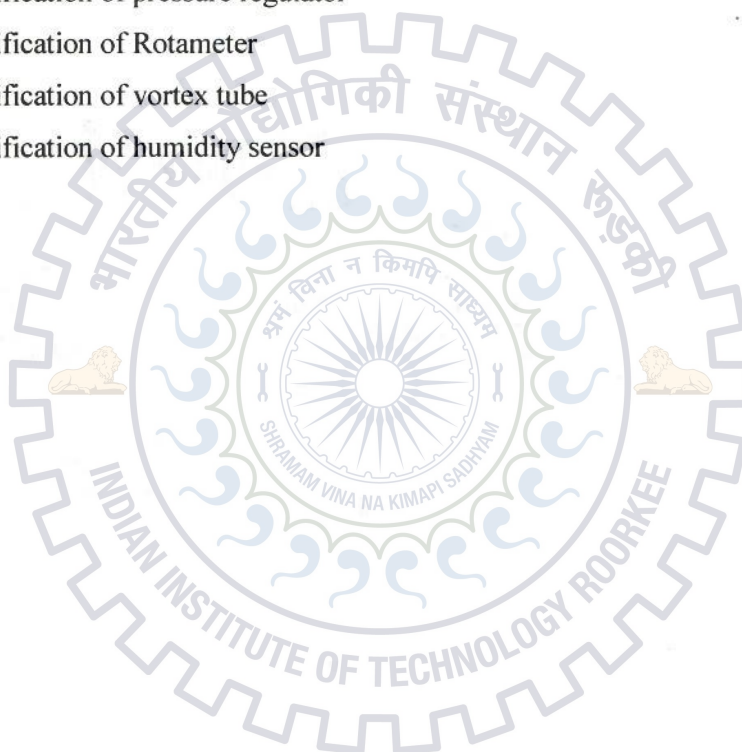
4.5.3	Variation of Reynolds number with cold mass fraction at different inlet pressure without insulation on vortex tube	48
4.5.4	Variation of Reynolds number with cold mass fraction at different inlet pressure with insulation on vortex tube.	49
4.6.1	Input pressure function of Reynolds number	49
4.6.2	Variation of cold mass fraction with Reynolds number	50
4.6.3	Variation of temperature drop with Reynolds number	50
4.7.1	Input pressure function of Reynolds number	51
4.7.2	Variation of temperature drop with Reynolds number without insulation	51
4.7.3	Variation of cold mass fraction with Reynolds number	52
4.7.4	Variation of non-dimensional temperature drop with cold mass fraction	53
4.7.5	Variation of non-dimensional temperature drop with cold mass fraction (insulation on vortex tube)	54
4.8.1	Variation of COP with cold mass fraction with insulation	55
4.8.2	Variation of COP with cold mass fraction without insulation.	55
4.8.3	Variation of COP with inlet pressure (without insulation)	56
4.8.4	Variation of COP with inlet pressure (with insulation)	56
4.8.5	Variation of COP with inlet pressure (with insulation) at fully closed control valve	57
4.8.6	Variation of COP with inlet pressure (with insulation) at 50 % closed hot control valve	57
6.1	Dead weight tester with pressure transducer	61
6.2	Showing calibration between pressure value in DAQ and pressure value in calibration system for transducer range (0-16 bar)	62
6.3	Showing calibration between pressure value in DAQ and pressure value in calibration system for transducer range (0-10 bar)	62
6.4	Calibration data with correlation for temperature	63
6.5	Calibration data with correlation for sensor 2	64
6.6	Calibration data with correlation for sensor 1	64

6.7	Calibration data with correlation for rotameter range 80-800 LPM	65
6.8	Calibration data with correlation for rotameter range 10-100 CFM	66
6.9	Variation of dynamic viscosity with temperature, and correlation equation	66



LIST OF TABLES

Table No.	Description	Page No.
1.1	Summary of few experimental studies on vortex tube	3
2.1	Researchers on vortex tube with different fluids	13
2.2	Moisture removal capacity using different gas	17
3.1	Specification of compressor	22
3.2	Specification of pressure regulator	24
3.3	Specification of Rotameter	25
3.4	Specification of vortex tube	26
3.5	Specification of humidity sensor	27



NOMENCLATURE

Symbol	Description
V_{bz}	Breathing zone outdoor airflow (cfm)
R_p	Outdoor airflow rate required per person (cfm/person)
P_z	Zone population
R_a	Outdoor airflow rate required per unit area (cfm/ft ²)
A_z	Zone floor area: the net occupiable floor area of the zone (ft ²).
CFM	Cubic feet per minute
DBT	Dry bulb temperature (°C)
RH	Relative humidity
TR	Tone of refrigeration (Watt)
h	Enthalpy (kJ/kg.K)
\dot{m}_a	Mass of air per sec
\dot{m}_w	Mass of water per sec
$\Theta_{in}-\Theta_c$	Temperature drop at cold end side (°C)
$\Theta_h-\Theta_{in}$	Temperature drop at hot end side (°C)
LPM	Liter per minute
\dot{m}_c	Cold mass flow rate (kg/s)
w	Work input to the compressor (Watt)
\dot{m}_{in}	Inlet mass flow rate (kg/s)
D	Diameter of vortex tube (mm)
C_p	Heat capacity at constant pressure (kJ/kg.K)
Θ_c	Cold end side temperature (°C)
Θ_h	Hot end side temperature (°C)
Psi	Per square inch
P	Pressure (bar)
F	Force (N)
A	Area (cm ²)
mA	Mili-ampere

J	Current density (A/m ²)
ΔV	Voltage difference (V)
E_{emf}	Electromotive force (Nm/ C)
S	See-beck coefficient
RHVT	Ranque Hilsch vortex tube
CFD	Computational fluid dynamics
CNC	Computer numerical control
CFCs	Chlorofluorocarbons
L	Length of vortex tube (mm)
Pa	Atmospheric pressure (bar)
DAQ	Data acquisition system
l	Length of room (foot)
b	Breadth of room (foot)
h	Height of room (foot)
d	Inlet diameter of nozzle (mm)
Re	Reynolds number
COP	Coefficient of performance
R	Characteristic gas constant (kJ/kg.K)

Greek letters

δ	Diameter of cold orifice (mm)
σ	Electrical conductivity (S/m)
μ	Dynamic viscosity of air (Pa.s)
v_1	Specific volume at outdoor condition (m ³ / kg)
Λ	Area of inlet nozzle (mm ²)
Σ	Non -dimensional cold temperature drop
Ψ	Non -dimensional hot temperature drop
Υ	Efficiency
\dot{r}	Specific heat ratio
κ_c	Cooling capacity (Watt)

- ω Specific humidity (kg of water vapor/ kg of dry air)
 Θ Temperature ($^{\circ}\text{C}$)
 Ω Mass fraction



INTRODUCTION

Thermal comfort in air conditioning is defined by ASHRAE handbook: 55 % relative humidity and 24 °C dry bulb temperature in psychometric chart. Average skin temperature of fully grown person is about 24.1 °C. Human body can gain or loss heat depending upon the ambient temperature. Body of person losses heat and eventually he feels grief, if ambient temperature is less than the average skin temperature. Body receives heat from outside and person feels uncomfortable if surrounding temperature is more than average skin temperature. Therefore we have to design air conditioning system around the alignment circle in psychometric chart, which is around the 55 % relative humidity and 24 °C dry bulb temperature. Thermal comfort is touched by external factors such as metabolic rate, air speed, and relative humidity and cloth insulation. Thermal comfort is also affected by single person presumption. Therefore thermal comfort for individual in given space or building is very difficult to achieve.

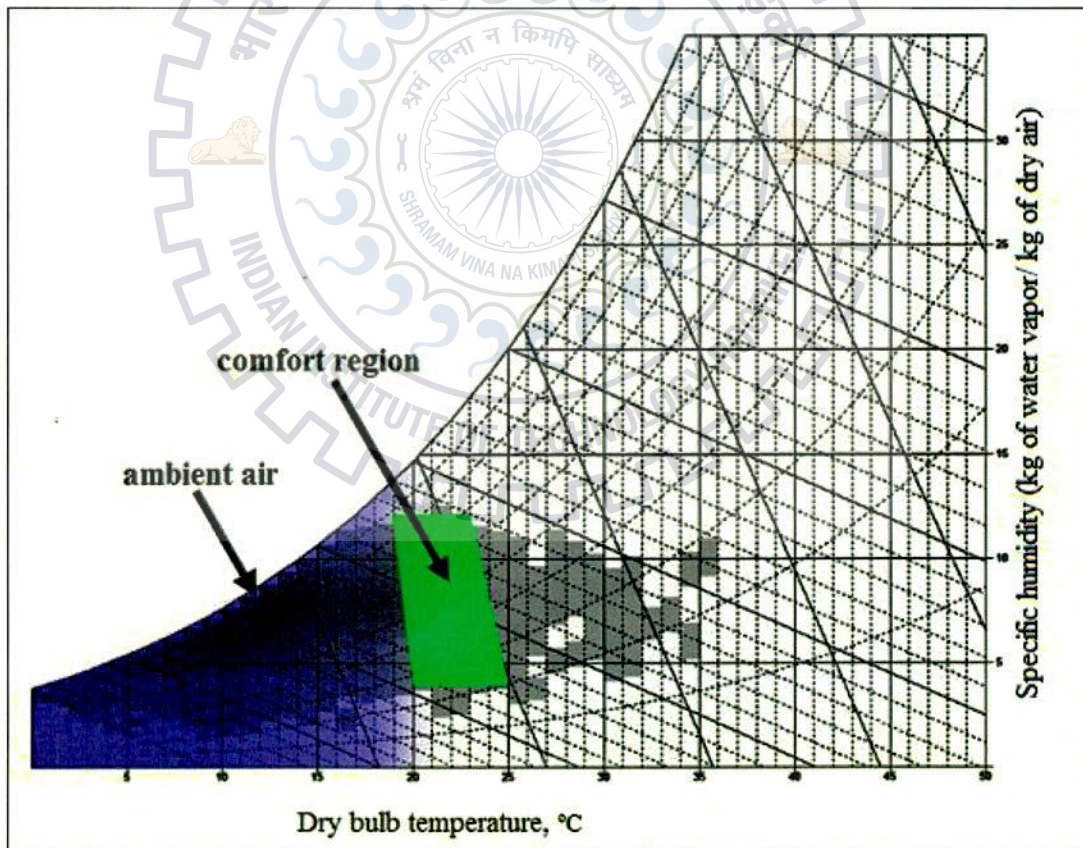


Fig.1.1: Psychometric chart showing comfort region [internet].

It includes heating, air conditioning and ventilation. When a person feels uncomfortable he can adopt to achieve thermal comfort for sometimes by non-energy consumable method, like cloths, indigenous fans, Sun and sunshades.

To achieve air-conditioning in the given space, we can use the Ranque – Hilsch vortex tube. By use of this, we can achieve very quickly the conditioned space and it has advantage over the traditional air conditioner. Vortex tube is simple and economical mechanical device which is used for splitting continuous flow of compressed gas from the compressor in to two parts. One of the part of gas exits at temperature less than the input temperature from small orifice near the inlet tangential nozzle, and remaining part of gas is leaving from far end of the vortex tube at temperature more than input temperature of compressed gas from the mass flow controlling device called throttle control valve. This effect of vortex tube is best known as a temperature separation effect. It is not very efficient for cooling of building, but further it is extensively used for industrial purpose like cooling of cutting tool, CNC machine, cooling of electronic part in aircraft, camera, and oil & gas exploring units. Reasons behind this vast application are its simple operation, less space required, less in weight, no moving part, therefore requires less or no hauling. It does not use any refrigerant as compared to traditional air conditioner which uses CFCs. Therefore it is eco-friendly and sustainable.

1.1 Historical background and progress work on vortex tube

Ranque [1, 2] was first discussed the vortex tube in the year 1932. In the early days, it was left for several years due to statements of scientist and committee was not good about this device. Because it does not compete in market due to its poor efficiency. Later Hilsch [3] show his interest in vortex tube and did large number of experiment in the year 1947 by considering parameters like its diameter, entry of nozzle, number of inlet, length of vortex tube, and inlet pressure. Hilsch explained correctly the effect happening in the tube, and his results give better efficiency.

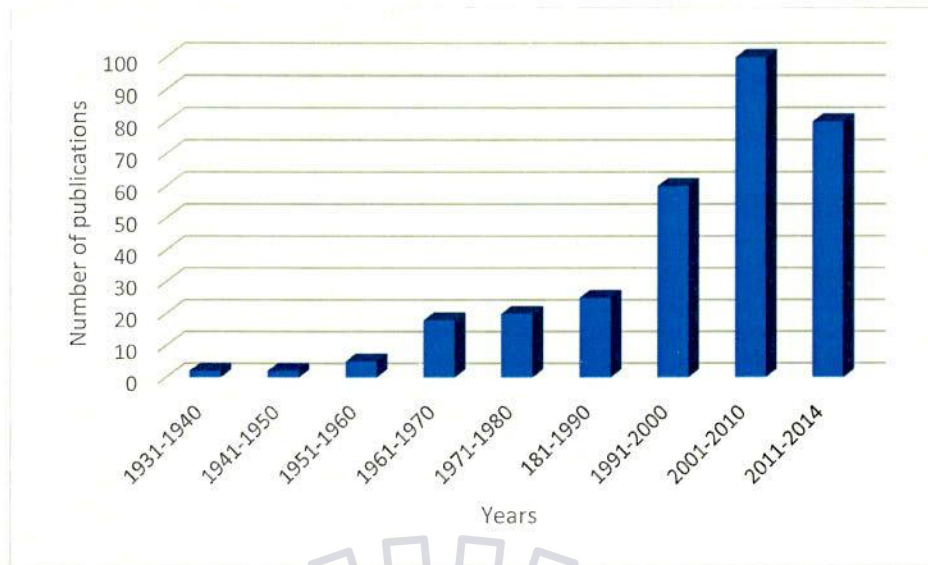


Fig.1.2: Number of publications [63].

Later Scheper [4] joined the Hilsch and by use of probe and visualization technique. He measured the pressure, total temperature and velocity in one directional vortex tube. Martynovskii and Alekseev [5] studied experimentally on design parameter of vortex tube. After the year 1947, it is very interested field for researcher especially large application point of view in industry.

Reason for getting cold temperature drop and hot temperature drop is very complex and not correctly explained by many researchers due to turbulent flow of working fluid in vortex tube.

Dobratz [6], Curley and McGree [7], Kalvinskas [8] did significant work to understanding the cause for getting cold and hot air from single compressed gas at predetermine temperature and pressure. He also studied on turbulent flow in vortex tube to forecast the trend of graphs by using some advanced tool like CFD, $k-\omega$ model, and he got some good results over the results obtained by researcher in early day of start of vortex tube for cooling of small cabin and small temperature difference applications.

Table.1.1: Summary of few experimental studies on vortex tube

Year	Investigator	Dia. (mm)	P_i (atm)	Ω_c	$\Theta_h - \Theta_i$	$\Theta_c - \Theta_i$
19933	Ranque	12	7	-	38	-32
1947	Hilsch	4.6	11	.23	140	-53
1951	Scheper	38.1	-	-	-	-

1956	Martynovskii and Alekseev	4.4/28	12	-	-	-40
1960	Takahama and Kawashima	52.8	-	-	-	-
1965	Takahama	28/78	-	-	-	-
1966	Takahama and Saga	28/78	-	-	-	-
1994	Ahlborn et al.	18	4	.38	40	-30
1996	Ahlborn et al.	25.4	2.7	.4	30	-27
2003	Saidi and Valipour	9	3	.6	-	-17.37
2005	Promvonge and Eiamsa-ard	16	3.5	.38	25	30
2005	Aljuwayhel et al.	19	3	.1	1.2	-11

1.2 Vortex tube

Vortex tube is consisting of circular tube of a straight length with throttle valve at hot end side, and nozzle tangentially near the small central hole called cold orifice. Specification of vortex tube is defined by the diameter of vortex tube (D), length of vortex tube (L), diameter of cold orifice (d), and number of nozzles. Ratio of mass flow rate is controlled by hot control valve i.e. cold mass flow fraction (Ω_c), and hot mass flow fraction (Ω_h). Orifice diameter should be half of the vortex tube for the best result.

Some useful terms which define the specification of vortex tube like cold mass fraction, cold temperature drop, coefficient of performance and isentropic efficiency are described.

Cold mass fraction Ω_c is ratio of amount of mass flow rate leaving at cold end to total amount of mass flow rate entering the vortex tube. It is very essential term to define the optimal performance of vortex tube. It can be changed by operating hot control valve at far distance from the position of inlet port.

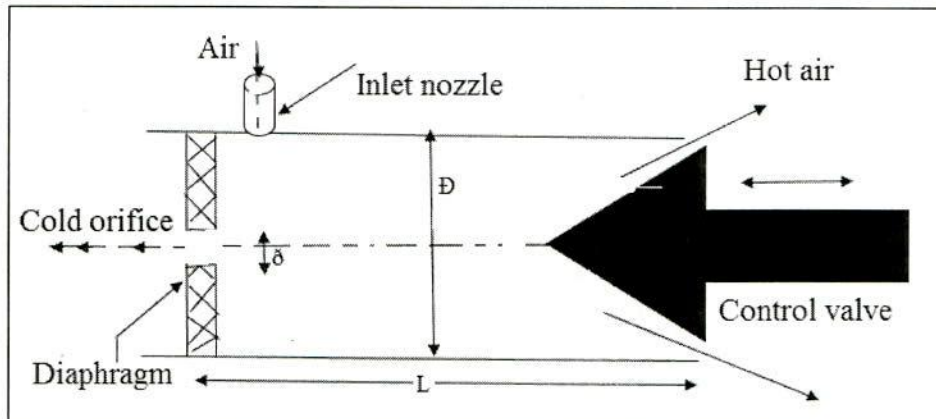


Fig.1.3: Vortex tube counter flow type.

1.3 Vortex tube parameter

1.3.1 Cold mass fraction Ω_c : It is very important parameter in study of performance of vortex tube, defined by ratio of mass flow rate (\dot{m}_c) leaving from cold orifice to the mass flow rate (\dot{m}_{in}) at inlet.

$$\Omega_c = \frac{\dot{m}_c}{\dot{m}_{in}}$$

1.3.2 Hot and cold temperature drop: To get cold air temperature drop, if we subtracts the cold temperature from inlet temperature. Similarly we can also obtain hot temperature drop, by subtracting inlet temperature from the hot temperature.

$$\Delta\theta_c = \theta_{in} - \theta_c, \quad \text{cold temperature drop}$$

$$\Delta\theta_h = \theta_h - \theta_{in}, \quad \text{hot temperature drop}$$

1.3.3 Coefficient of performance: Coefficient of performance of vortex tube is defined as ratio of cooling capacity to the work input to the compressor.

$$COP = \frac{\kappa_c}{w},$$

κ_c = Cooling capacity,

w = Compressor work

$$w = R \left(\frac{\dot{\gamma}}{\dot{\gamma}-1} \right) \theta_{in} \left[(P_a / P_i)^{\left(\frac{\dot{\gamma}-1}{\dot{\gamma}} \right)} - 1 \right]$$

$$\text{Cooling capacity} = \Omega_c C_p \Delta \theta_c$$

1.3.4 Cooling efficiency: To check the performance of vortex tube, it is required to calculate next term, isentropic cooling efficiency. Ideal gas law is used to calculate efficiency based on the constant temperature expansion. Compressed air enters the vortex tube and expands adiabatically up to temperature θ_s .

$$\gamma_{\text{isentropic}} = \frac{\Delta \theta_c}{\theta_{in} - \theta_s}$$

$$\gamma_{\text{isentropic}} = \frac{\Delta \theta_c}{\theta_{in} \left[(P_a / P_i)^{\left(\frac{\dot{\gamma}-1}{\dot{\gamma}} \right)} - 1 \right]}$$

$\dot{\gamma}$ = heat capacity ratio,

P_a = atmospheric pressure

P_i = pressure at inlet

1.3.5 Reynolds number: It is defined as ratio of inertia force to the viscous force.

Mathematically,

$$Re = \frac{\dot{m} d}{4 \Lambda \mu}$$

\dot{m} = inlet mass flow rate (kg/sec)

d = diameter of inlet nozzle (10 mm)

Λ = area of inlet nozzle (mm²)

μ = dynamic viscosity of air (Pa.s)

1.3.6 Non-dimensional temperature drop: It is defined as ratio of temperature difference between cold / hot temperature and input temperature to the input temperature.

Mathematically,

Non-dimensional cold temperature drop

$$\Sigma = \frac{\theta_c - \theta_{in}}{\theta_{in}}$$

Non-dimensional hot temperature drop

$$\Psi = \frac{\theta_h - \theta_{in}}{\theta_{in}}$$

1.4 Types of vortex tubes

Vortex tubes are categories mainly in to two parts on taking account of direction of working fluid flow.

1.4.1 Counter flow vortex tube

Fig.1.4 shows schematic diagram of counter flow vortex tube. Air enters tangentially in to vortex chamber with the help of nozzle. Vortex tube separates incoming air in to two parts; one part at low temperature leaving at orifice and remaining part at high temperature leaving from the hot valve. Flow of working fluid travels opposite to each other within the tube. Therefore its name is coined by counter flow vortex tube.

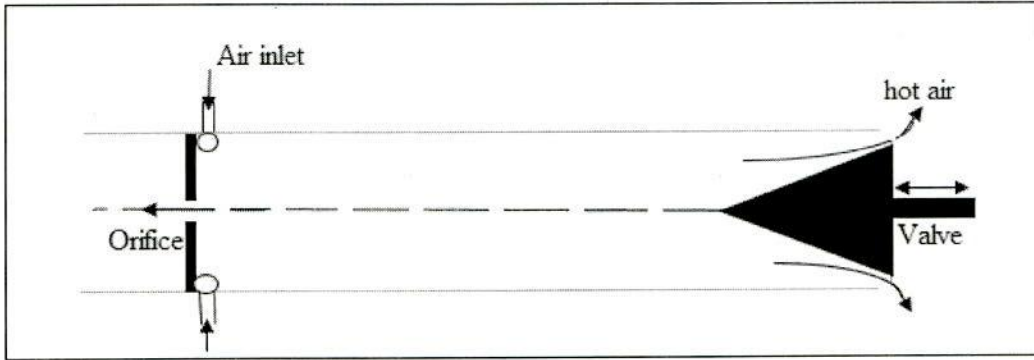


Fig.1.4: Counter flow vortex tube.

1.4.2 Parallel flow vortex tube

In parallel flow vortex tube, compressed air passes in to vortex tube by means of nozzle near the fully closed end of the tube. Hot air leaving from other end of the tube along the surface of control valve. It consists of concentric control valve. Cold air travels by concentrically control valve and finally comes in to atmosphere. This type of vortex tube is not very effective for application purpose.

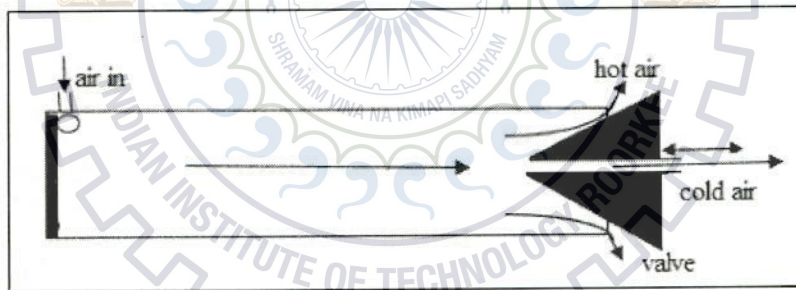


Fig.1.5: Parallel flow vortex tube.

1.5 Applications of vortex tube

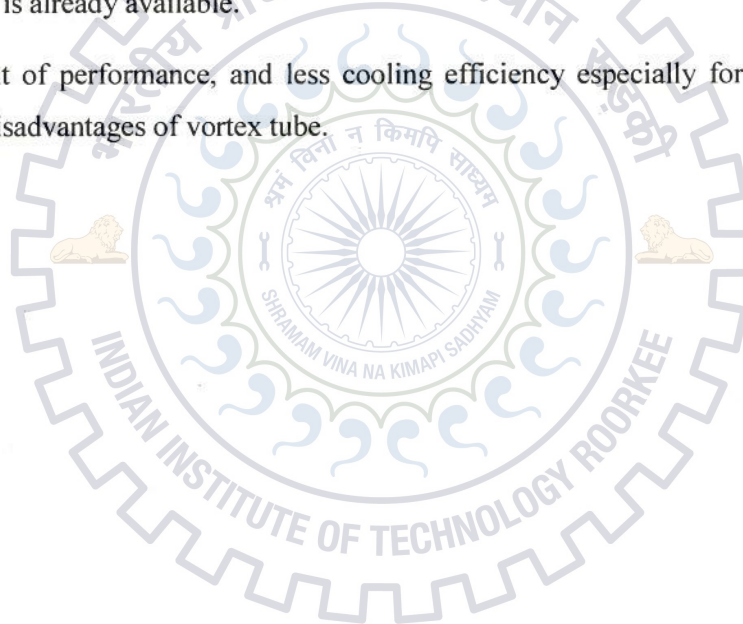
Its efficiency and coefficient of performance is not very good, even though it may very useful device in present and in future for industrial purposes. This device is most widely important for industrial applications. It is helpful for cooling of cutting tool in cutting process and also removing simultaneous chips from material surface. Other applications are cooling of electronic parts, braze spot, making of water from atmospheric air, cooling of test temperature sensor, air

dehumidification, making of ice. It may be also used in gas and oil exploration industry, and utilizes waste energy discharge at more than atmospheric pressure, separation of gas particle from gas industry, cooling of small space cabin [9], low pressure applications [11] and body cooling of worker in fire [10] and mines [12] industry.

1.6 Advantages and disadvantages of vortex tube

Vortex tube has many advantages over a convention refrigeration machine due to its simplicity in design and no requirement of large control system, no or little maintenance because of no moving parts. It is light in weight thus acquire less space, and most efficient and less cost where compressed air is already available.

Low coefficient of performance, and less cooling efficiency especially for large space, noisy operation are disadvantages of vortex tube.



LITERATURE REVIEW

In this chapter, details of vortex tube, reasons for temperature separation, details about experimental setup, measurements of pressure and temperature, moisture content in air after leaving from the cold side of vortex tube will be discussed. The detailed explanations about experiment and experimental results done by large number of publishers in this field will be reviewed and discussed.

2.1 Working principles of Ranque- Hilsch vortex tube

Ambient air is compressed by reciprocating compressor and stored in tank. Compressed air enters vortex tube by single or more nozzles. Incoming air achieves high speed before splitting in to two parts due to shape and design of nozzle. Air flows in spiral path along the diameter of vortex tube by creating vortex flow inside the vortex space. Working principles are explained theoretically and experimentally by Yunpeng Xue et.al. [13]. Vortex tube forcibly separates continuous flow of air in to two parts. First part of the stream at temperature lower than at which air enter, near the nozzle from small round hole called cold orifice. Remaining part of air is warmer due to wall friction and compression, leaving from the control valve along the periphery of tube. Mass flow rate of air from cold end and cold temperature are controlled by placing valve at hot end side of vortex tube.

2.2 Mechanism

Main part of vortex tube is cylindrical pipe as shown in Fig.2.1. Leaving of splitting stream is either made in one end or both ends of the vortex tube. Hot control valve is located at the far end and cold orifice located at center line of the tube. The compressed gas under high pressure is injected tangentially in to the vortex tube by helping of one or more than one nozzle. The vortex flow is generated inside the chamber.

Compressed gas flows towards the wall surface of the chamber due to centrifugal force, therefore a frictional force (shear stress) developed near the wall surface and flow becomes warm. The vortex tube is fully hollow and no part inside, therefore temperature separation is occurred within it due to some fluid or thermodynamics effect. Warm gas leaving from periphery of the tube at temperature higher than inlet temperature and center part of the gas which is back force by control

valve is expelled from cold orifice. While the cold stream of gas is simultaneously generated near the cold orifice due to radial expansion along the centerline of vortex chamber.

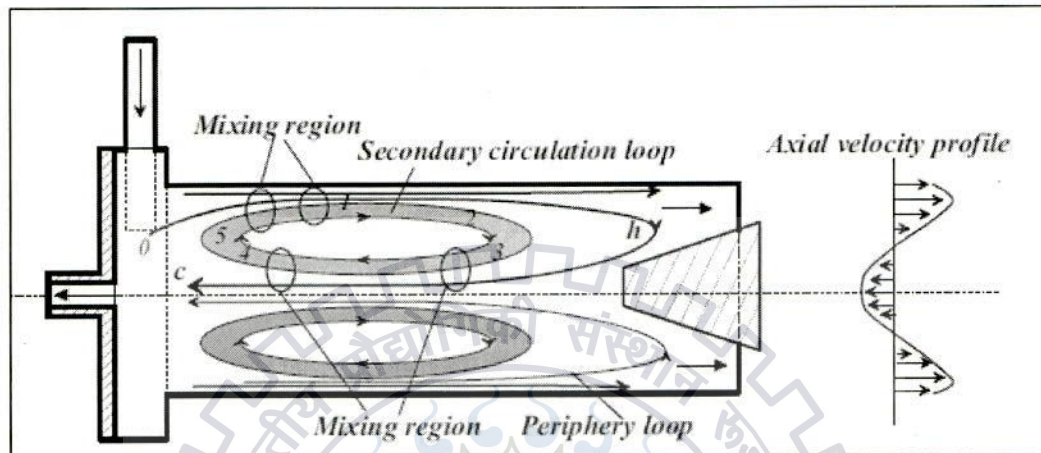


Fig.2.1: Secondary circulation [14].

Temperature difference in RHVT is called temperature separation or energy separation. Energy separation is occurred due to energy transfer from central core flow to outer peripheral flow [14]. Small amount of the inner flow mixed with multi-circulation and forms small vortices. These vortices help to separates cold flow and multi- circulation. Ahlborn et al. in 1994 [15, 16] investigated and concluded during experiment that pressure gradient existing inside vortex tube creates lowest temperature in the region of central core flow near the inlet nozzle. Phenomenon of temperature separation in vortex tube is unexpectedly discovered by Ranque in 1931. Later Hilsch improved the performance of RHVT by studying the various geometrical parameters and thermo physical parameters.

2.3 Temperature drop in vortex tube

Temperature drop in vortex tube by Ranque [1] is due to adiabatic expansion and compression of working fluid. Later Gutsol [17] explained that it is due to centrifugal separation of air and adiabatic expansion of incoming air in vortex tube. Performance of vortex tube analyzed by Lewins and Bejan [18] by considering above two statements; adiabatic expansion and another centrifugal

flow of air. In order to know the cause behind the temperature drop in vortex tube, we have to first check what process occurring inside tube. This is explained by Xue et al. [19] using flow identify technique. Concept of flow circulation was given by them in which part of central flow moved outwards and back to the hot end. Cold air produces near the inlet nozzle due to sudden expansion of air. Hot flow is generated due to partial stagnation of flow at hot end.

Takahama [20] gave the general idea about nature of flow inside tube which behaves as force vortex. Groves [21] added his work to Takahama by measuring axial and radial velocity and told free vortex exit at periphery and force vortex flow at the centerline of vortex tube. To remove difficulty of measurement of flow inside tube, Gao et al. [22] measured temperature, pressure and 3-D velocity pattern. Dincer et al. [23, 24] did investigation by exergy analysis considering the different nozzle and working fluid like methane, air, oxygen, nitrogen.

Aljuwayhel et al. [25] and Behera et al. [26] investigated and explained the concept of temperature separation by transfer of heat between layers of fluid. Due to viscous shear, heat transfer is possible. Behera et al. [26] investigated the temperature separation in vortex tube using CFD code star – CD on length of tube and secondary circulation was considered. Eiamsa-ard and Promvonge [27, 28, and 29] did experiments and observed large temperature gradient near the wall of tube, and temperature process is high in the core flow near the nozzle.

Hilsch [2] investigated and stated that air leaving from cold orifice losses its kinetic energy due to internal fluid friction. Air enters tube at high pressure at periphery of tube and after expansion, air attains low pressure at axis of tube. It is reason for air losses most kinetic energy from centerline flow to outer flow. Therefore air leaving at cold orifice is at lower temperature and remaining air exhausting from control valve at higher temperature. Simoes-Moreira et al. [30] stated that expansion of entering air is driving cause for getting hot and cold flow.

Ramakrishna et al. [31] stated that temperature separation is due to shear work transfer. Shear work transfer is work associated with the friction between fluid layers caused by high speed rotating fluid surface which produces torque.

A new type of vortex tube were introduce by Eiamsa-ard S.A et.al. [52], called double circuit vortex tube, with conical tube to increase the performance. In this type of vortex tube, an orifice is placed at center of hot control valve. Gas at same inlet temperature is introduced through this

orifice at lower pressure. Cooling efficiency of vortex tube increased and also performance was improved. Guillaume et al. [51] investigated on two stage vortex tube and obtain more temperature drop from single vortex tube. Air exit from the cold side was introduced in to second vortex tube at same operating condition.

Table 2.1: Researchers on vortex tube with different fluids.

Year	Researchers	fluid	Results
1957	Martynovskii V.S., and Aleksiev V.P [5]	Ammonia ,CH ₄ , CO ₂	When Pr < 0.5, hot fluid flow from cold exit and cold fluid flow from hot end. This phenomenon was not explained and discussed.
1971	Williams A. [32]	Methane rich mixture	At given pressure and low temperature air is liquefied in the tube, and separation effect reduces.
1979	Collins R.L. and Lovelace R. B. [33]	Two phase propane	Inlet pressure P _{in} = 0.791 MPa and quality
1988	Balmer R.T [34]	water	At P _{in} = 20-30 MPa. And obtain all outlet temperature higher than inlet temperature.
1995	Jin H. and Ji G. [35]	Two phase flow consisted air and water	Vortex tube with water also has the temperature drop effect
1997	Keller J.U. and Gobel M.U. [36]	R22, R134a,R7 44	COP of system using R22 ,R134a and R744 increased by 5%, 10%, 2.5% respectively
2003	Poshernev N.V. and	Natural gas	Result are same as Williams [35]

	Khodorkov I.L. [37]		
2005	Cao Y. et al. [38]	N ₂ , Ne, He	Fluid of small thermal conductivity enhance the temperature drop.
2006	Dincer K. et al. [39]	O ₂ , N ₂ ,CO ₂	Compared with O ₂ and N ₂ attain lower temperature.
2006	Aydin O. et al. [40]	Air , O ₂ , N ₂	Molar mass of N ₂ is smaller than molar mass of O ₂ . Thus its temperature drop is better.

Later Ahlborn et al. [16] in 2009 introduced a new theory to explain the concept of temperature separation as the classical thermodynamics cycle with adiabatic expansion and adiabatic compression. Arbuzov et al. [57] stated that Ranque effect inside the vortex tube due to viscous heating of the gas in the thin boundary layer near the wall of tube and adiabatic cooling of the gas near center. Williams [42] proposed another application of vortex tube in making of ice. It is also use for dehumidifying the air and also removal of water from air.

Another explanation of temperature separation is thermal separation due to energy transfer from inner flow to outer flow. It has been investigated that inner flow rotates at lower angular velocity than peripheral flow. Therefore loss in angular momentum of core flow results as transfer of kinetic energy to the outer flow as axial movement of vortex flow. Temperature of peripheral flow increases as gain of heat transfer and temperature of inner flow decreases due to loss of kinetic energy. But none of the explanation is entirely satisfying the phenomenon of temperature separation due to its complex flow behavior within the vortex tube.

2.4 Vortex tube as classical refrigeration cycle

An investigation was carried by Jeffrey M. Gordon et al. [41] and explained the vortex tube as a classical refrigeration cycle. Region near the inlet nozzle, warm gas in secondary circulation transfer heat in to cooler gas in primary circulation. Williams D.T. [42] explained working fluid enters the vortex tube at high speed, high pressure and moves towards the hot end nozzle and again comes back towards the core central flow. In this region gases are expanded. Mechanical energy

gained from axial movement of compressed gas therefore this mechanical energy is utilized to push secondary circulation radially outwards. Vortex tube very quickly reached steady state and also time independent temperature profile is obtained. Therefore, there is no change in internal energy of gas in full cycle which is requirement of any thermodynamics cycle.

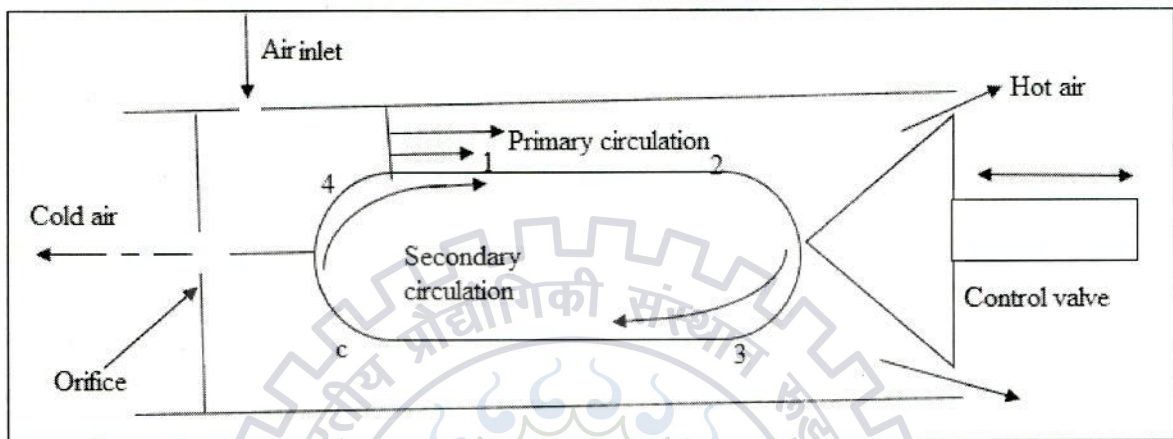


Fig.2.2: Vortex tube as refrigeration cycle.

2.4.1 Heat rejection process (4-1): Warm gas in the secondary circulation flow delivers heat to the cold gas in the primary flow. Coldest region in vortex tube is near nozzle entry, where gas expanded adiabatically from higher pressure to lower pressure. At point 4 swirl velocity is much more than radial and axial velocity. It means part of secondary and primary circulation travel side by side for long path.

2.4.2 Adiabatic expansion (1-3): High pressure air in vortex tube travels towards the hot end and turn back to join centerline flow. Therefore pressure at point 2 is more than the pressure at point 3. Secondary circulation flow expands adiabatic due to pressure difference.

2.4.3 Heat absorption process (3-c): In this process air flow along centerline cool by transferring energy to the periphery flow. Both flow is in motion due to strong swirl velocity, momentum transfer between flow and small scale mixing cold flow. Therefore cold flow experience more fluid friction in vortex tube as compare in simple pipe. Air in primary loop continuously delivers energy to the secondary flow and cool down.

2.4.4 Adiabatic compression process (c-4): Mechanical energy due to axial velocity help to move forward secondary circulation and compressed toward the point 4. This process is known as adiabatic compression and temperature of secondary flow increase from temperature at temperature.

Vortex tube consider as thermodynamics cycle for air conditioning in which different process occurs compression, expansion, heat rejection and heat absorption. It acts as natural heat exchanger device. With the help of Pressure, Temperature, Velocity and cold mass fraction we analyze the performance of vortex tube. Flow field inside vortex tube is very complex in nature and difficult to explain the concept of temperature or energy separation inside vortex tube. There are several researchers did experiments and try to explain the basic reason for obtaining two temperature one at lower temperature and another at higher temperature from single injection of air. But no one gave the correct explanation of temperature separation and phenomenon occurring inside vortex tube is still unclear.

2.5 Study on Ranque-Hilsch vortex tube for the moisture removal

Large amount of energy required for any drying process in industry. With the help of vortex tube we can reduce the amount of heat required. Therefore large interest on vortex tube of engineers is to minimize the energy required. Large amount of compressed gas is exhausted from many industrial operations. Ranque- Hilsch vortex tube may be used as device to recover some exhaust gas at pressure above atmospheric, by heating and cooling of small range temperature variation for given space.

Stanescu G et al. [43, 44] did an investigation and explained that if exhausted gas from many industrial process at even low pressure but required mass flow rate then its waste energy is also utilized. Main objective of Stanescu G et al. [43, 44] was to increase the performance of RHVT for recovering the waste energy at some useful pressure for cooling and heating and increasing the air moisture removal. He found air moisture removal capacity 0.024-0.05 (kg water vapor/ kg of dry air) at pressure range 0.3- 0.7 MPa. It was found that methane gas has high capacity of moisture removal.

Table 2.2 Moisture removal capacity using different gas

Working Fluid	Pressure Range	Moisture Removal Capacity (kg water vapor/ kg of compress air)
CO ₂	0.3-0.7 MPa	0.024-0.05
Air	-	30
Methane	-	80

Amitani et al. [45] concluded that temperature separation is due to compressibility of working air. Lindstrom Lang [46] stated that turbulent flow of thermal energy is incompressible flow. Temperature separation is totally dependent upon the type of gas used in vortex tube. Heating and cooling in vortex tube is due to conversion of either energy into heat or heat into energy; increase the hot temperature drop $\Delta\theta_h$ and decreasing the cold temperature drop $\Delta\theta_c$.

Westley R. [47] and Shamsoddini R. et al. [48] did a numerical investigation and found number of inlet nozzle is very important that change the performance of vortex tube. It helps to keep uniform velocity. Investigation was found with more number of nozzle capable to obtain more temperature drop. CFD model is a very powerful tool in these days which not only improves the analysis accuracy but also increases the performance of vortex tube and easily evaluates what happens inside the vortex tube. To manipulate behavior of flow inside tube, two techniques were used by [27] [28] RSM turbulent model and k- ω model. If we increase the cost of accuracy and computational then k- ω model is better than other CFD model.

The physical flow variables like temperature drop, pressure distribution and velocity profile were analyzed and was found that cold temperature drop depends on the diameter of orifice. Most accurate results were found at diameter 0.7 mm. Results are evaluated at different diameters and found that cold temperature drop and hot temperature drop is obtained due to angular momentum transfer and kinetic energy transfer.

2.6 Droplet behavior in Ranque-Hilsch vortex tube

Vortex tube is mainly used for cooling purpose but also used for removing non-condensing component from the mixture of different gas. Behavior of droplet inside vortex tube were investigated by R Liew et al. [49] using MATLAB model. Model uses Lagrangian approach for droplet in space and time coordinate. Force acting on the swirl flow for droplet condensation or evaporation are defined according to kinetic energy transfer from centerline flow to periphery flow. Results were observed if humidity at inlet of vortex tube increases, concentration of droplet increases. More droplet will be collided when concentration of droplet increases and therefore liquid easy to separate.

Droplet are spherical and treated as Lagrangian particle. This particle does not change nature of flow. There are two types of forces acting on the flow; first is viscous frictional force and second is centrifugal force due to rotating nature of flow. Other forces were neglected in this study because density of gas is much lower than droplet of liquid. When N_2 gas is used in vortex tube, droplet is evaporated. This is due to different partial pressure and to overcome this effect, first N_2 gas need to dehumidify. Due to change in centrifugal forces both evaporation and condensation affect the formation of droplet. This investigation was done by Sazhin et al. [50].

2.7 Geometrical factors affecting the performance of Ranque-Hilsch vortex tube

There are many factors that affect the temperature drop in vortex tube and also influences on its performance. Many researchers did investigations on parameters including diameter and length of tube, size and shape of inlet nozzle, vortex chamber, diameter of cold orifice and hot control valve. Takahama [53], [54], [55] and Soni [56] published few papers on this topic consisting relationship between parameter of vortex tube and performance of tube.

2.7.1 Humidity

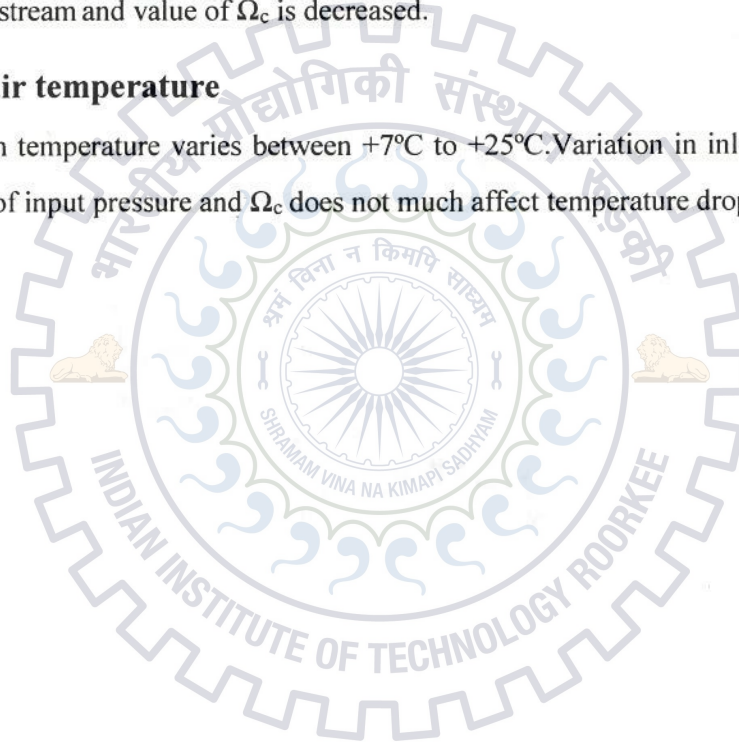
If the moisture presenting in the air is entered then it reduces the efficiency of vortex chamber in refrigerant due to heat transfer to the cold air stream by condensation and formation of water vapor which change the phase. Generally there is decrease in vortex effect when the tube is operating with moisture in liquid state.

2.7.2 Compressed air pressure

Increasing compressed air pressure at inlet of vortex tube increases the temperature drops $\Delta\theta_c$ and $\Delta\theta_h$ of the air stream and value of Ω_c is decreased.

2.7.3 Input air temperature

Input air stream temperature varies between $+7^\circ\text{C}$ to $+25^\circ\text{C}$. Variation in inlet temperature with constant value of input pressure and Ω_c does not much affect temperature drop $\Delta\theta_c$, $\Delta\theta_h$.



EXPERIMENTAL METHODOLOGY AND SETUP

Purpose of present work is to find out the effects of the cold mass fraction Ω_c , inlet pressure and Reynolds number on the temperature difference i.e. cold temperature drop and hot temperature drop, and relative humidity (RH) by using Ranque- Hilsch vortex tube. Working fluid air is used for evaluating these parameters. To obtain these thermo physical properties, we use pressure transducer, relative humidity sensor, pressure regulator, air rotameter, T- type thermocouple and data acquisition system.

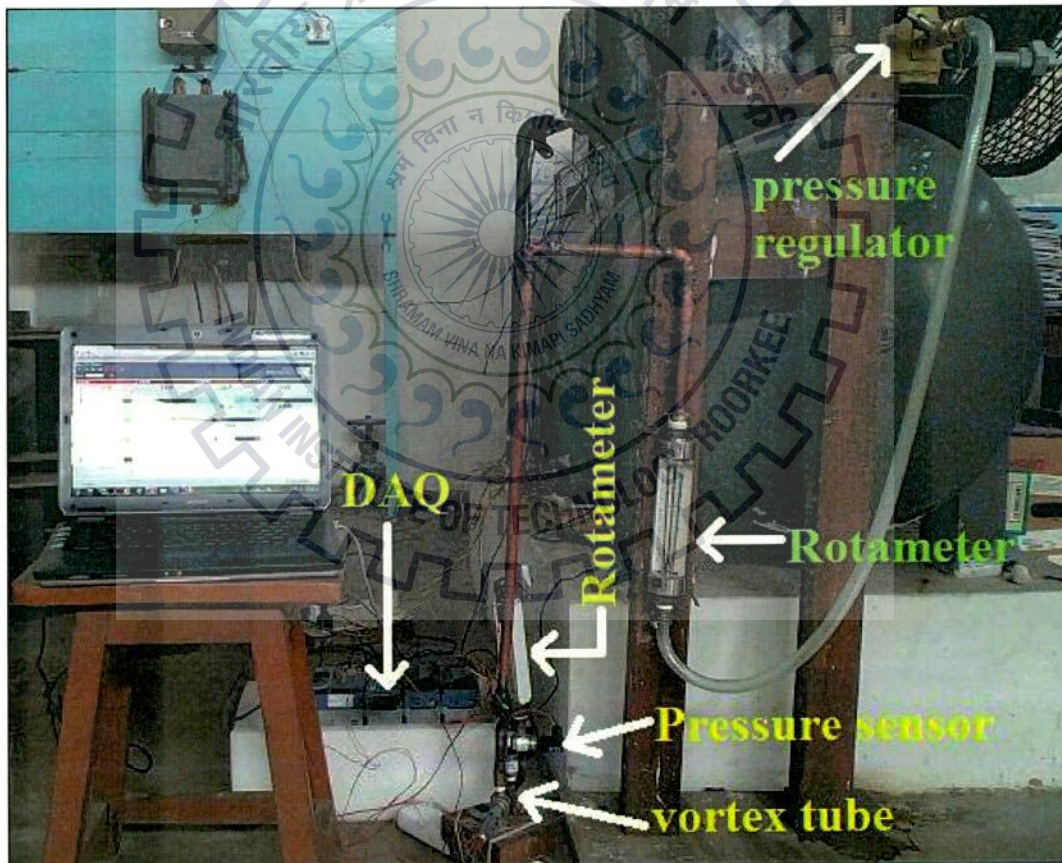
3.1 Experimental setup

Fig.3.1: Photographic view of experimental setup.

A photographic view of experimental setup is shown in above Fig.3.1. It is used to calculate all desired physical properties. Experimental setup is consisting of a pressure regulator, some fittings, and two pressure transducers, two rotameters, two humidity sensors and few T-type of thermocouples.

3.1.1 Air compressor

Air compressor shown in Fig.3.2 is a device that convert power using electrical energy in to potential energy to store pressurized air in storage tank. By several methods, air compressor is pumping air more and more in to storage tank or supply line. Energy stored in tank can be used in various industrial applications. We get kinetic energy when tank is depressurized. In our experiment, we use low pressure compressor having discharge pressure up to 200 psi. It is a reciprocating compressor. First it take the atmospheric air from the ambient and there is auto cut off and compressor stop when it reaches 150 psi. We assume approximation isothermal compression of working fluid by compressor.

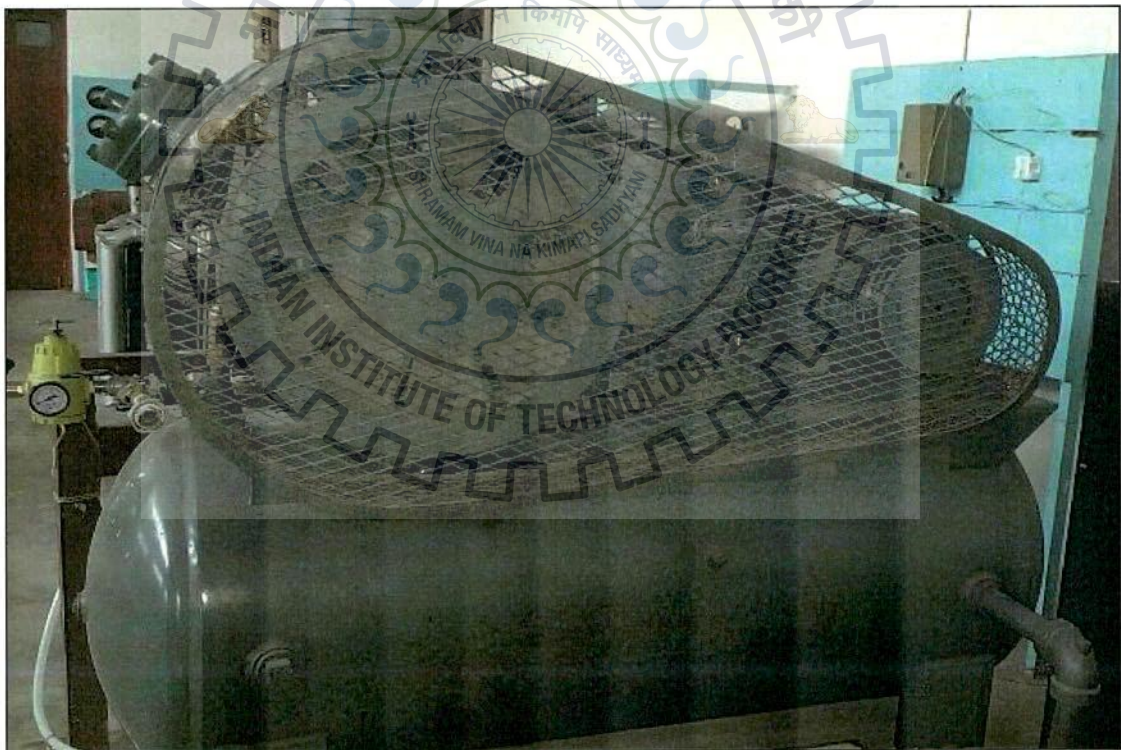


Fig.3.2: Reciprocating air compressor.

Table 3.1: Specification of compressor

Parameters:	Values:
Maximum working pressure	200 psi
Design pressure	200 psi
1 bar =14.50 psi	psi = “per square inch”
Number of cylinders	2

3.1.2 Pressure regulator

Single stage pressure regulator is consisting of a single diaphragm and a needle valve. High pressure gas enters in to the regulator through inlet valve in to chamber. Pressure is indicated by the pressure gauge fitted on the regulator. Gas fills the high pressure chamber completely. Needle valve remains closed without any interference. High pressure gas remains contained in the valve chamber. When the adjusting knob turn clockwise it compresses the spring and exerts the downward force on the diaphragm and it pushes the valve to open. This releases the gas from high pressure chamber to low pressure chamber exerting upward force on the diaphragm.

Equilibrium is reached when spring force is equal to the combined upward force exerted by needle spring, gas in high pressure chamber and low pressure chamber. When the regulator is in use, initial pressure start to drop. The reduced pressure in the valve chamber means lessor upward force of the high pressure gas in the valve chamber acting on the valve. Thus total combined upward force of gas in the low pressure chamber. The upward exerted force on the valve spring and upward force of the high pressure gas in valve chamber acting on the valve is becoming lower than the downward force on the diaphragm exerted by the spring.

Now there is lower upward force on the diaphragm than the downward force exerted by spring,so the diaphragm travels further downward making the valve further open to allowing more gas to fill the low pressure chamber and hence there is increase in outlet pressure as indicated by the outlet pressure gauge. Once the cylinder is empty, inlet gas flow becomes shut off and outlet pressure becomes zero.



Fig.3.3: Air pressure regulator.

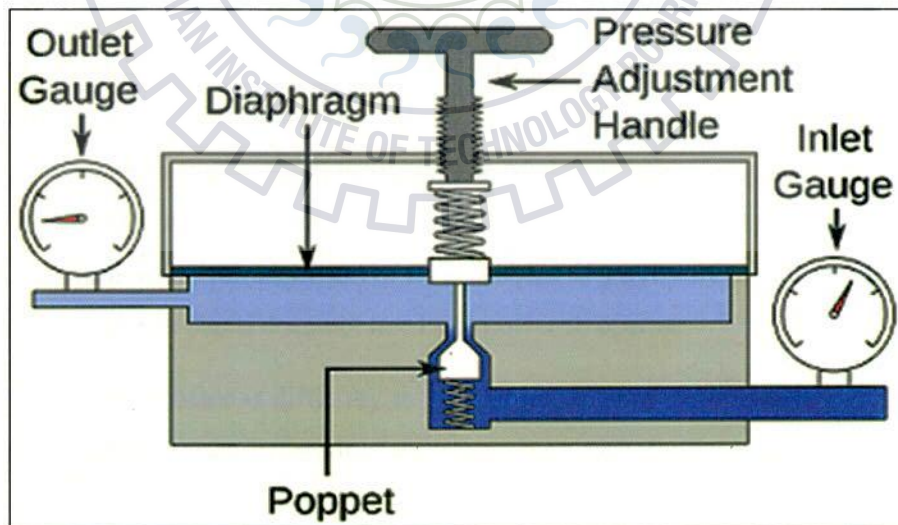


Fig.3.4: Inside view of air pressure regulator [internet].

Table 3.2: Specification of pressure regulator

Parameters:	Values:
Pipe line size	½" taper thread
Body material	Aluminum alloy die cast
Adjustment	Non-rising metal knob
Maximum inlet pressure	20 bar
Maximum output pressure	10 bar
Maximum operating temperature	80 °C
Standard nominal flow	126 SCFM
1 SCFM	28.345 LPM
SCFM = specific cubic feet per minute	LPM = liter per minute

3.1.3 Rotameter

Rotameter is a device used to measure flow rate of a given fluid in a closed tube. It consists of a tapered glass tube and float. Float is pushed up by drag force of the flow and pulled down by the gravity. It is worked on the principle of varying area principle. A metal float is raised by flowing fluid in tapered pipe. It is always put in vertical position, area increasing from bottom to top. Height of float in glass tube is indicated the flow rate. In case of liquid rotameter, the float is raised by both buoyancy force and velocity head. While in case of air rotameter, buoyancy forces neglected and only velocity head is responsible to indicate the value of flow rate. After few seconds, float is stable in the glass tube when velocity head of flow is equal to gravity force due to weight of float. Advantage of Rotameter is that it does not need any power to operate.

Disadvantage of the Rotameter is difficulty to read exact value of flow rate. In this experiment, two Rotameter are used; one at before inlet of vortex tube and another at cold exit of tube, for finding mass flow rate.

Table 3.3 Specification of Rotameter

Parameters:	Values:
Number of Rotameter	2
Working fluid	air
Body	transparent solid acrylic block
Operating pressure range	1-10 bar
Maximum range	80 – 800 LPM ,10 – 100 CFM
Float	SS316
Inlet	bottom
Outlet	top
Mounting size	1/2" ,1"



Fig.3.5: (a) Air rotameter (CFM) at inlet.



Fig.3.5: (b) Air rotameter at (LPM) cold exit.

3.1.4 Vortex tube

Vortex tube is a mechanical device used as refrigeration unit without using refrigerant and energy. It consists of straight tube, inlet nozzle, orifice and hot control valve.

Table 3.4 Specification of vortex tube

Parameters:	Values:
Model	50015H
Flow rate	283 – 1133 SLPM
Cross sectional area of cold exit	1.54E-6 m ²
Cross sectional of hot exit	7.85E-6 m ²
Tube length	157.5 mm
Input pressure range	1 – 7 bar
Inlet diameter of vortex tube	10 mm



Fig.3.6: Vortex tube.

3.1.5 Humidity sensor

Humidity sensor is required in our experiments for study and analysis of relative humidity after cold air leaves from orifice and inlet of vortex tube. Atmospheric air is mixture of different gases such as nitrogen, oxygen, hydrogen, carbon dioxide, water vapor, organ and small amount of other gases. Ambient air is not a pure substance due to mixture of dry air and water vapor. Therefore we requires more than two known parameters for evaluation of property of moist air. But we have only two known parameters; pressure and temperature, which are not enough for analytical calculation of property. In psychometric chart, variation in relative humidity with dry bulb temperature are plotted at constant pressure (standard atmospheric pressure $P = 1\text{atm}$).

Table 3.5 Specification of vortex tube

Parameters:	Values:
Temperature	- 40 to125 °C
Product series no.	HTG3515CH
Number of unit	Two, one at inlet, and another at cold exit of vortex tube.
Supply voltage	5 volt DC supply
Humidity range	0 to 100 % RH
Maximum power	25 mV

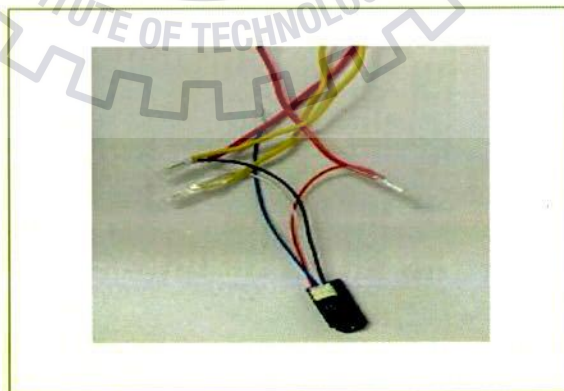


Fig.3.7: Humidity sensor (HTG3515CH).

Black wire is connected to negative of battery source.

Red colure wire for RH output.

White wire for positive terminal of battery source.

3.1.6 Pressure transducer

An electronic pressure sensor (PX2CG1XX016BSCHX), line connection 1/4” is used to measure pressure at inlet of the vortex tube. Its accuracy is 0.25% and operating temperature is -40 to 125 °C. Its range is from 0 to 16 bar (absolute) and it needs 5 to 30 V DC battery connection to sense the output value. Output of sensor is in the form of current in the range from 4 mA to 20 mA. DAQ (Yokogava) reads input only in voltage form. Therefore there is a need to add 250 k Ω resistance in series to convert output of sensor into the voltage form. Our DAQ system reads voltage signal and then convert it into require parameter. It is shown in Fig.3.8 and also in line connection diagram in Fig.3.9.



Fig.3.8: Electronic pressure transducer.

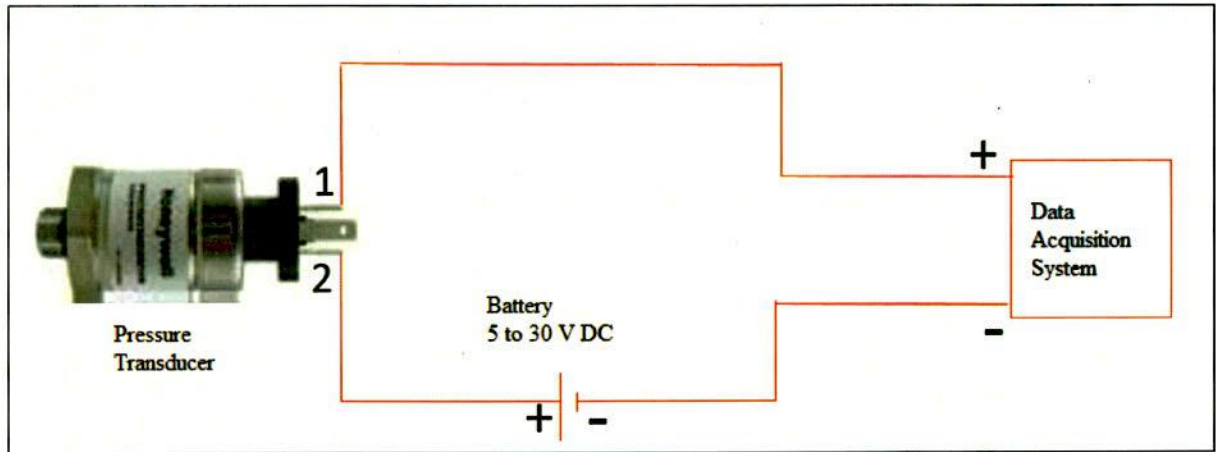


Fig.3.9: Line connection of transducer.

3.2 Experimental procedures

Schematic diagram of experimental setup is shown in Fig.3.2. First, air is compressed by reciprocating type compressor. Here we assume compression process of air isothermal. Compressed air is stored in tank at high pressure (150 psi). Before the compressed air enters the vortex tube, we set constant pressures like 1, 1.5, 2, 2.5, 3 bars etc. by using the pressure regulator. Here we use counter flow vortex tube. Compressed air from tank enters in to vortex tube by radial nozzle and creates swirl flow then it is split in to two flows; one at low temperature and another at high temperature. Temperature is measured by thermocouple (T- type) at an inlet, cold orifice and one at hot end of vortex tube. By pressure transducer (PX2CG1XX016BSCHX) measure absolute pressure at inlet of vortex tube. There are two Rotameters used; one at inlet and another at cold exit of vortex tube to measure the mass flow rates (kg/s). Mass flow rates are controlled by rotating control valve at the end of vortex tube.

Quantities of moisture present in compressed air are measured by two humidity sensors (HTG3515CH). One at before the inlet of vortex tube and another is placed at the exit of the cold flow from the orifice.

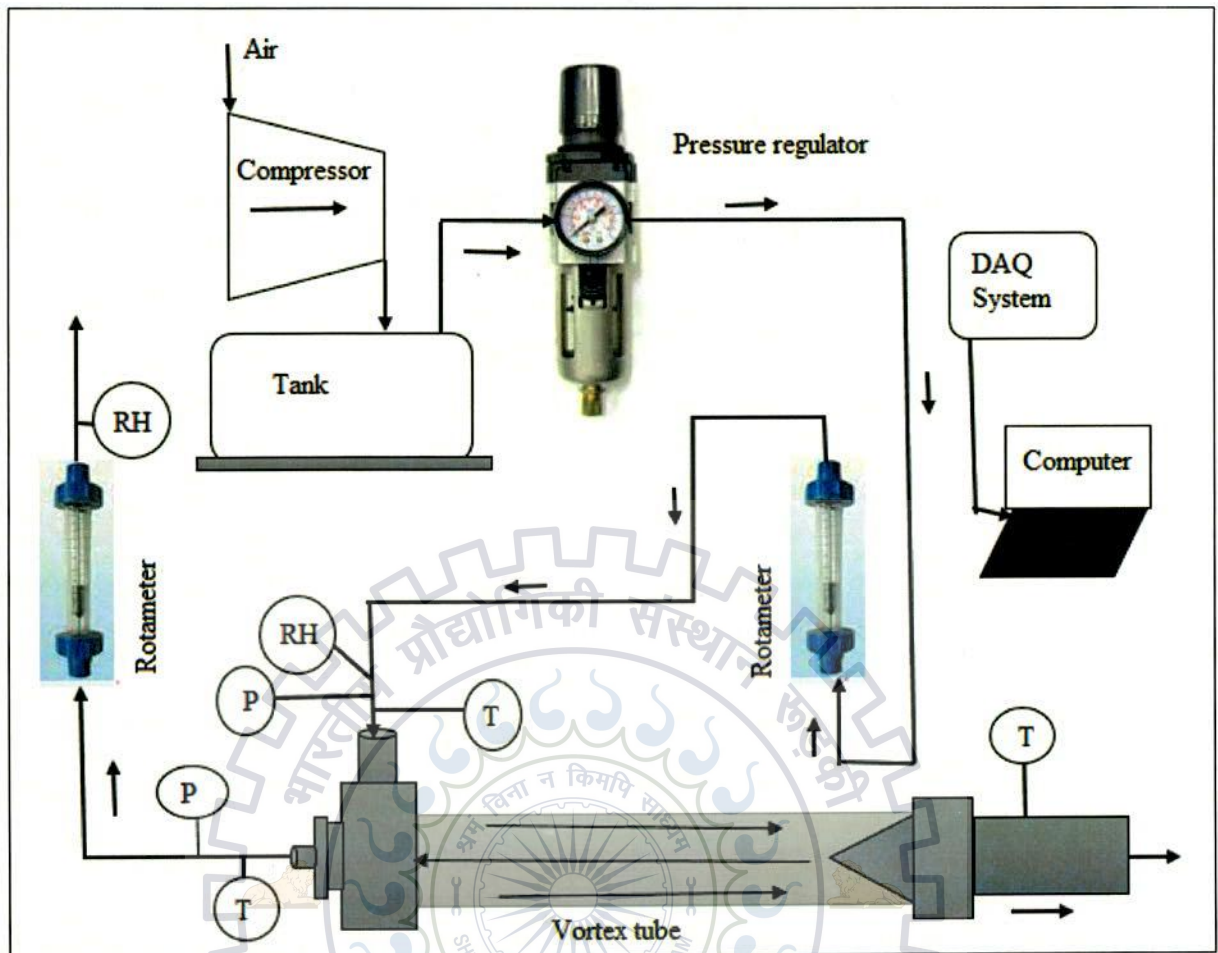


Fig.3.10: Schematic diagram of experimental setup.

T – Temperature sensor

P- Pressure transducer

RH- Relative humidity sensor

RESULTS AND DISCUSSIONS

In this chapter, all the results obtained from the experiments conducted are discussed.

4.1 Variation in hot and cold temperature drops, RH with cold mass fraction

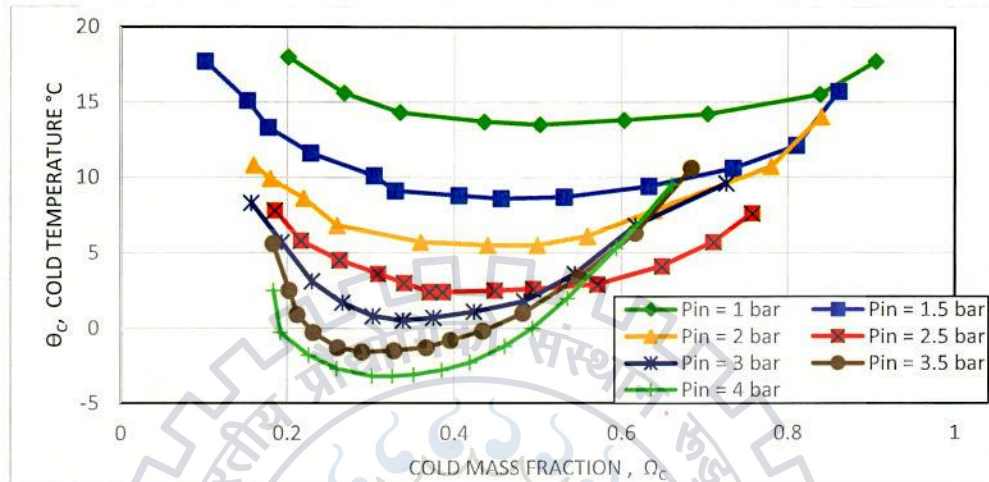


Fig.4.1: Cold temperature v/s cold mass fraction plot at different inlet pressures without insulation on vortex tube.

Duspara M. et al. [61] found maximum cold temperature of $-8\text{ }^\circ\text{C}$ at 4 bar. We get maximum cold temperature of $-4\text{ }^\circ\text{C}$ at 4 bar inlet pressure, without insulation. When insulation is used, we get $0\text{ }^\circ\text{C}$ at 4 bar.

From Fig.4.1, initially cold temperature (Θ_c) decreases when cold mass fraction increases from 0 to 0.5. It is due to Ranque [1] effect in which compressed air expands adiabatically near the orifice. But after ($\Omega_c > 0.5$) cold temperature increases. It is due to part of hot flow turn back and join the centerline flow. Therefore cold flow would gain energy from hot flow and become heated. A similar pattern is obtained at different constant inlet pressures. But graph is shifted toward the horizontal axis at high pressure, and getting negative cold temperature with the increase of pressure.

Similar pattern is obtained when experiment is done by using glass wool as an insulating material, wrapped all around over the vortex tube to minimize heat loss from surface of vortex tube shown in Fig.4.2. In this case we get less cold temperature as compared with the vortex tube without

insulation. For cold mass fraction for $\Omega_c < 0.5$, we get optimum value of cold temperature, while for without insulation at pressure $P_{in} = 1$ bar get optimum value for $\Omega_c = 0.50$. With insulation, part of hot flow get heated early and affect the temperature of cold flow, and it results lower temperature of cold flow leaving from orifice because there is no heat losses to ambient.

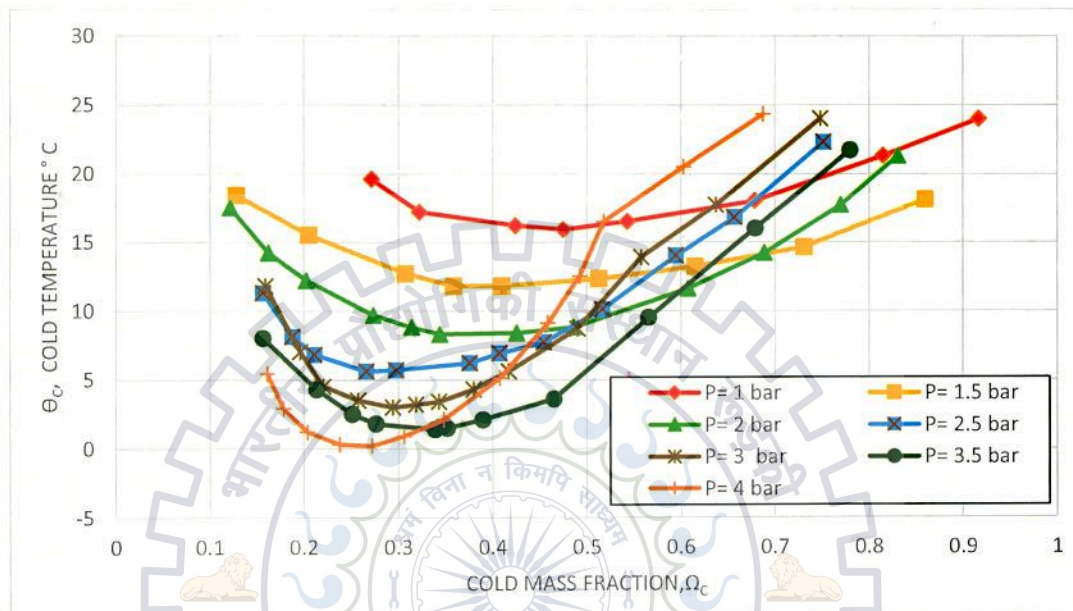


Fig.4.2: Cold temperature v/s cold mass fraction plot at different inlet pressure with insulation on vortex tube.

Variation in hot temperature, Θ_h is shown in Fig.4.3 against the different values of cold mass fractions, Ω_c . This graph is plotted without insulation on vortex tube. Hot temperature at the hot end increases with the increase in cold mass fraction. It is because of compression of air near the hot end explained by Ranque [1]. It is not only due to compression of air but also due to fluid friction between layer of fluid, momentum exchange, wall friction, secondary circulation and mixing of turbulent flow air leaving from hot end get heated. The plot is obtained at various input constant pressures, $P_{in} = 1, 1.5, 2, 2.5, 3$ etc.

Similar kind of graph is also obtained for vortex tube when insulation used shown in Fig.4.4. Hot flow transfer more energy to cold flow when cold mass fraction reaches ($\Omega_c > 0.6$) and eventually hot fluid cooled down by some degree of temperature. Therefore this is reason for getting less hot

temperature when insulation were used in vortex tube. Because thermocouple sense the temperature of hot fluid, only effect of convection happens when Ω_c reaches toward maximum.

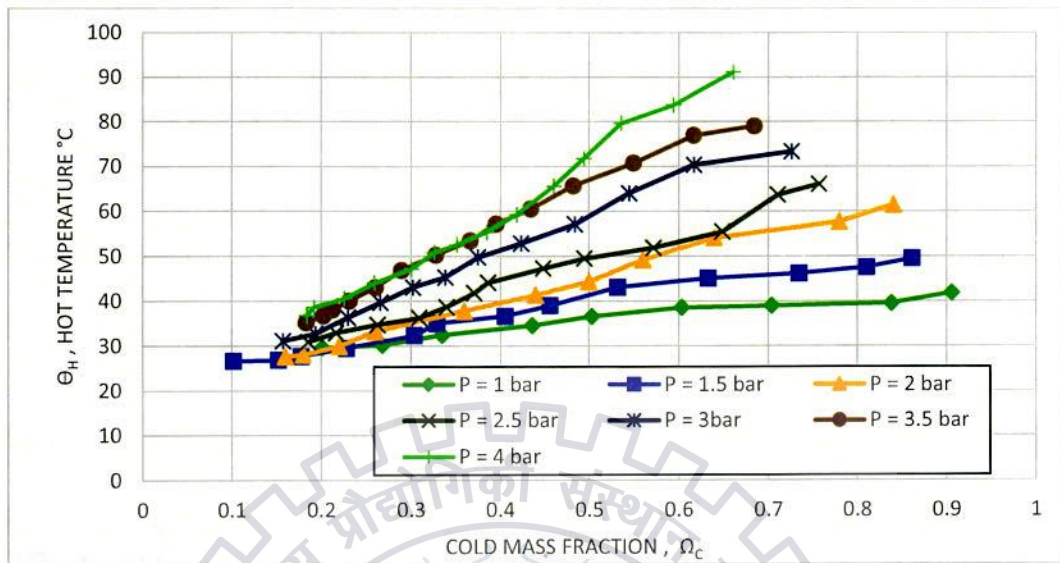


Fig.4.3: Hot temperature v/s cold mass fraction plot at different inlet pressure without insulation on vortex tube.

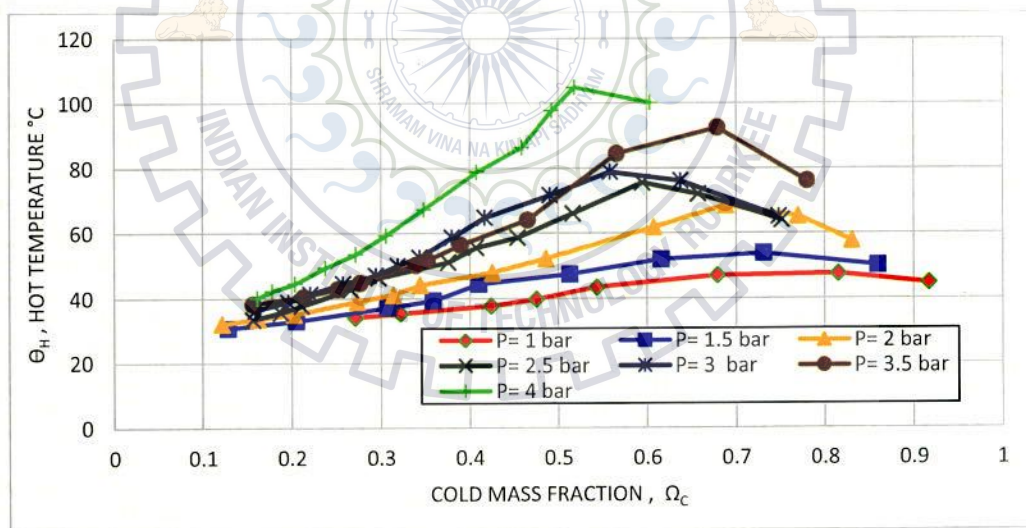


Fig.4.4: Hot temperature v/s cold mass fraction plot at different inlet pressure with insulation on vortex tube.

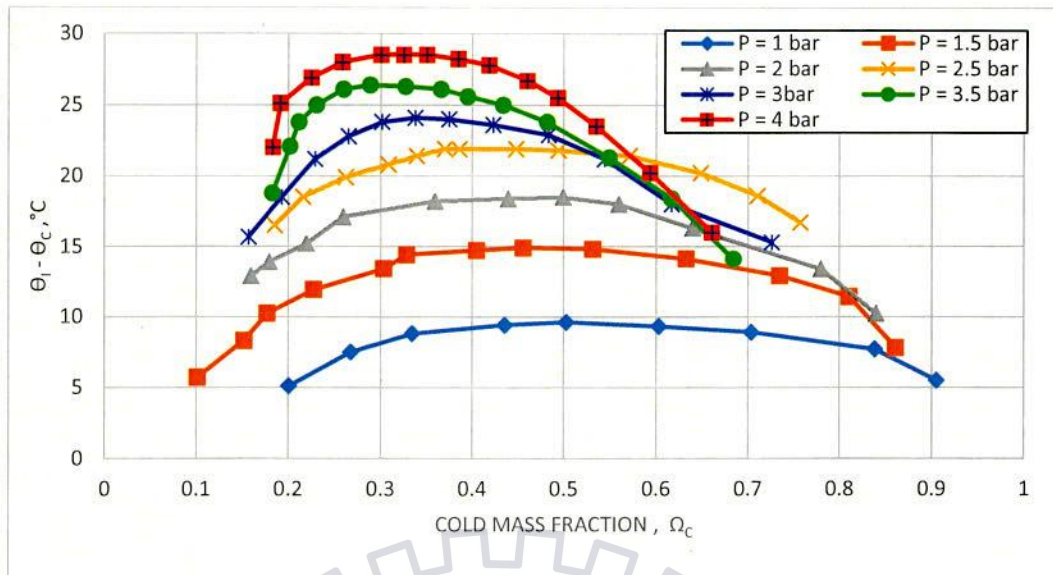


Fig.4.5: Cold temperature drop v/s cold mass fraction plot at different inlet pressure without insulation on vortex tube.

Fig.4.5 shows the variation of cold temperature drop ($\Theta_i - \Theta_c$) $^{\circ}\text{C}$ with the cold mass fraction. First cold temperature drop increases with the increase in Ω_c and then trend of graph fall. Optimal range of Ω_c is between 0.3 and 0.5 at high pressure and for low pressure its range are beyond $\Omega_c > 0.5$. Hilsch [3] found maximum cold temperature drop 15 $^{\circ}\text{C}$ at 2 bar inlet pressure at cold mass fraction range 0.3-0.4. We get maximum cold temperature drop 18 $^{\circ}\text{C}$ at 2 bar inlet pressure at cold mass fraction of 0.4 ~0.5. Promvonge et al. [52] found maximum value of cold temperature drop 17 $^{\circ}\text{C}$ at 2 bar inlet pressure. Agrawal N. et al. [60] found maximum cold temperature drop of 27 $^{\circ}\text{C}$ at 3 bar pressure. We get maximum value of 24 $^{\circ}\text{C}$ at 3 bar inlet pressure.

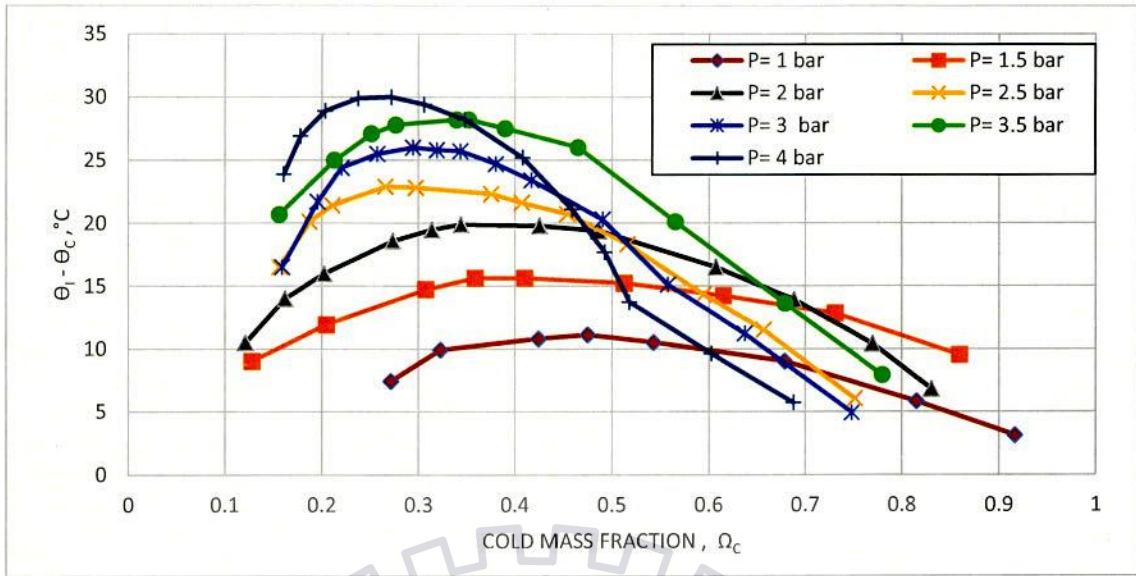


Fig.4.6: Cold temperature drop v/s cold mass fraction plot at different inlet pressure with insulation on vortex tube.

And similar pattern is obtained for with insulation shown in Figure 4.6. Optimum value of cold temperature drop at high pressure $P_{in} = 4$ bar is near 30°C . In Fig.4.6 we get maximum cold temperature drop of 20°C at 2 bar inlet pressure at cold mass fraction of 0.35~0.50.

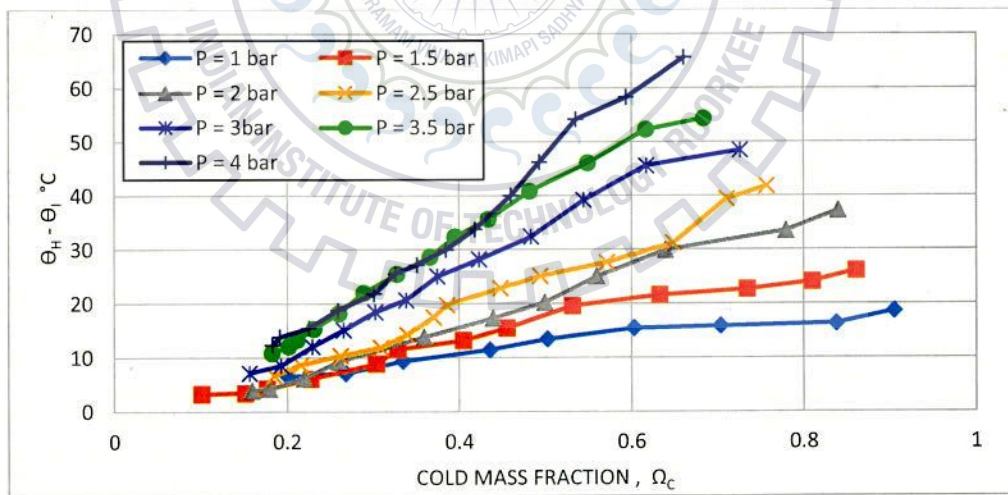


Fig.4.7: Hot temperature drop v/s cold mass fraction plot at different inlet pressure without insulation on vortex tube.

Mohammad S. V., and Nima N. [59] found maximum hot temperature drop of 32 °C at pressure 3 bar. We found maximum hot temperature drop of 50 °C at pressure 3 bar. When insulation used on vortex tube we get maximum hot temperature drop of 75 °C at 4 bar inlet pressure.

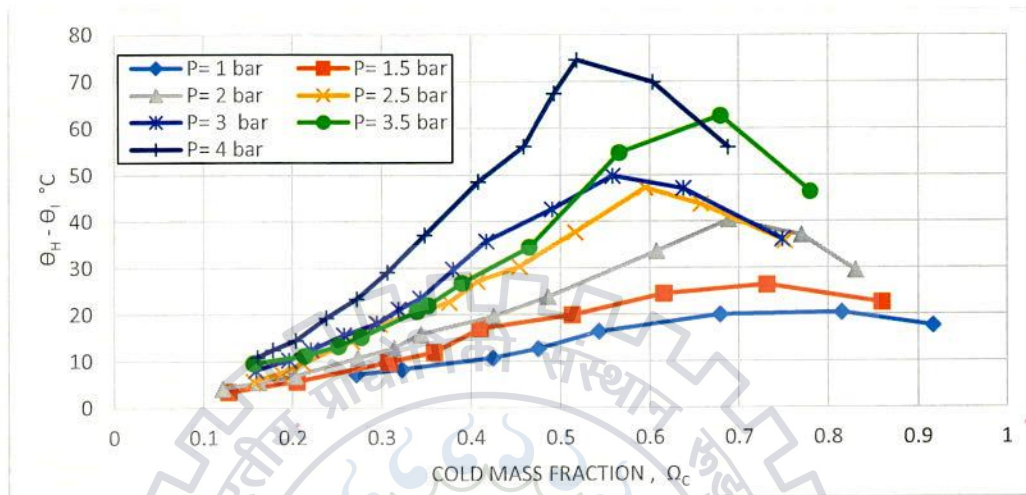


Fig.4.8: Hot temperature drop v/s cold mass fraction plot at different inlet pressure with insulation on vortex tube.

Eiamsa-ard S. et al. [29] found maximum hot temperature drop of 13 °C and 18 °C at 2 and 3 bar inlet pressure respectively. We get maximum hot temperature drop of 40 °C and 50 °C at 2 and 3 bar pressure respectively when insulation is in use.

Figure 4.9 shows the change in relative humidity with the variation of cold mass fraction Ω_c . Solid line represents relative humidity (%) at inlet of vortex tube and broken line indicates the relative humidity of cold flow leaving from the orifice. At $P_{in} = 1$ bar, humidity at inlet almost straight line up to cold mass fraction 0.6 and then increases up to $\Omega_c = 0.9$.

Humidity increases after cold mass fraction of 0.6 and it is due to accumulation of more water droplet because hot control valve in position of more closed. Air after leaving from cold orifice get dehumidified because its temperature falls and humidity almost constant. But when we increase the inlet pressure, relative humidity increases at inlet and cold exit of the vortex tube.

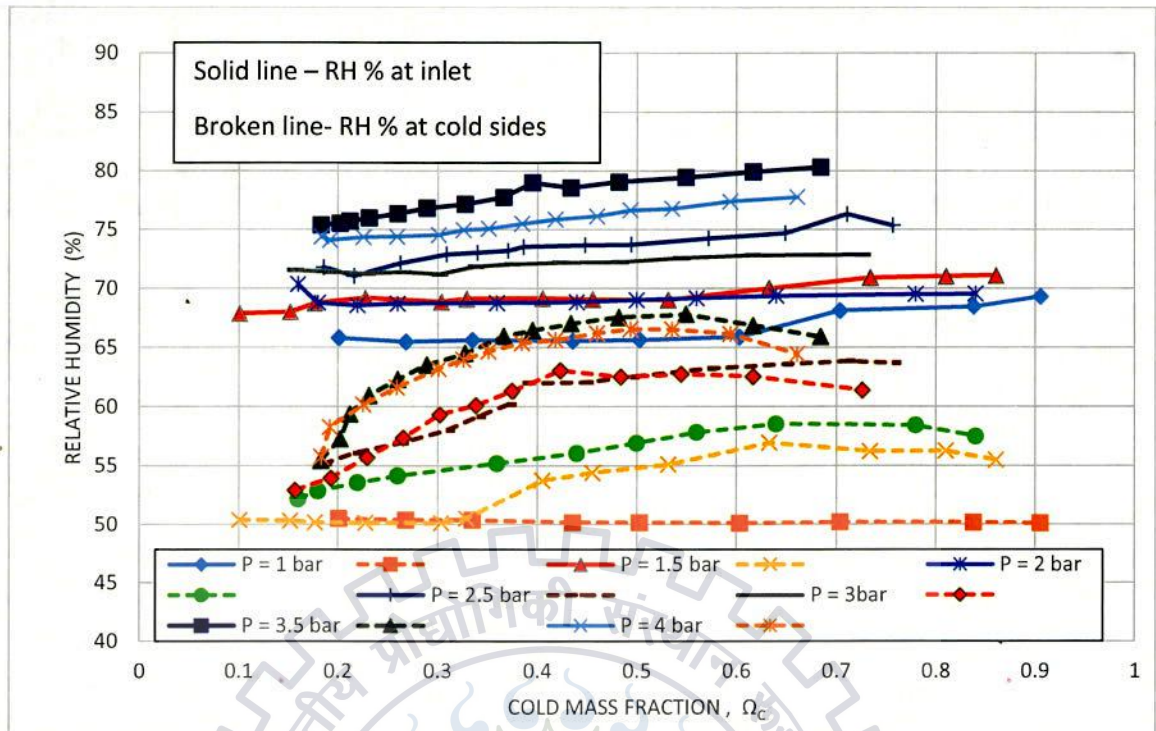


Fig.4.9: Variation of relative humidity with cold mass fraction at various input pressure without insulation used on vortex tube.

Humidity is very sensitive to temperature and velocity of air. Therefore it is reason for increasing humidity at increasing the pressure. But air dehumidify at the exit of air. From above figure relative humidity of air at high pressure first increase to optimum range of cold mass fraction $\Omega_c = 0.2 \sim 0.5$. After $\Omega_c \geq 0.5 \sim 0.6$ relative humidity decreases.

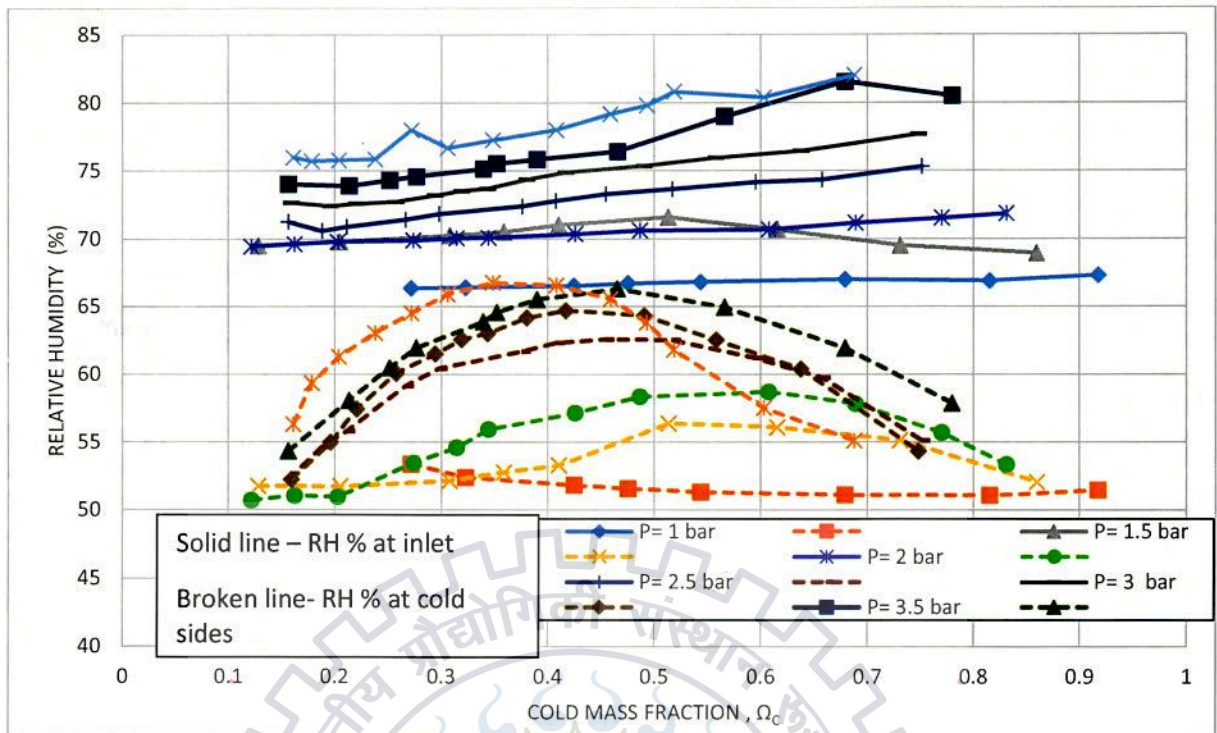


Fig.4.10: Variation of relative humidity with cold mass fraction at various input pressure when insulation used on vortex tube.

4.2 Analysis of thermo physical properties at fully open control valve

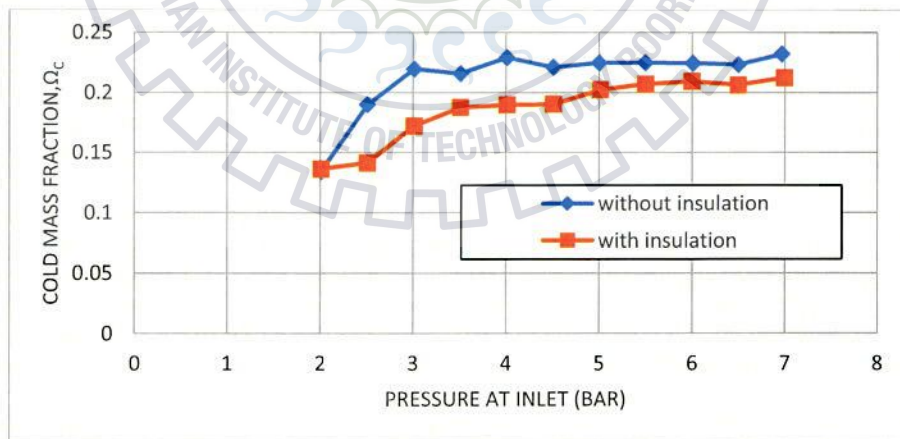


Fig.4.2.1: Variation of cold mass fraction Ω_c with various inlet pressure.

Fig4.2.1 shows the variation in cold mass fraction Ω_c and inlet pressure (absolute). Cold mass fraction increases with the increasing input pressure. Curve with insulation lies below from curve without insulation. It is because of more cold temperature drop occur with insulation, which decrease the density of cold fluid and eventually reduce the value of cold mass fraction. Also temperature of inlet air in case of without insulation were 23 °C to 25 °C, while in case of with insulation inlet temperature 27 to 30 °C. Difference in inlet temperature affect the value of inlet mass flow rate which is higher for without insulation. But cold mass fraction is lower than that of non-insulation.

Cold temperature decreases when inlet pressure increases for both cases with and without insulation. Fig.4.2.1 shows the above statement.

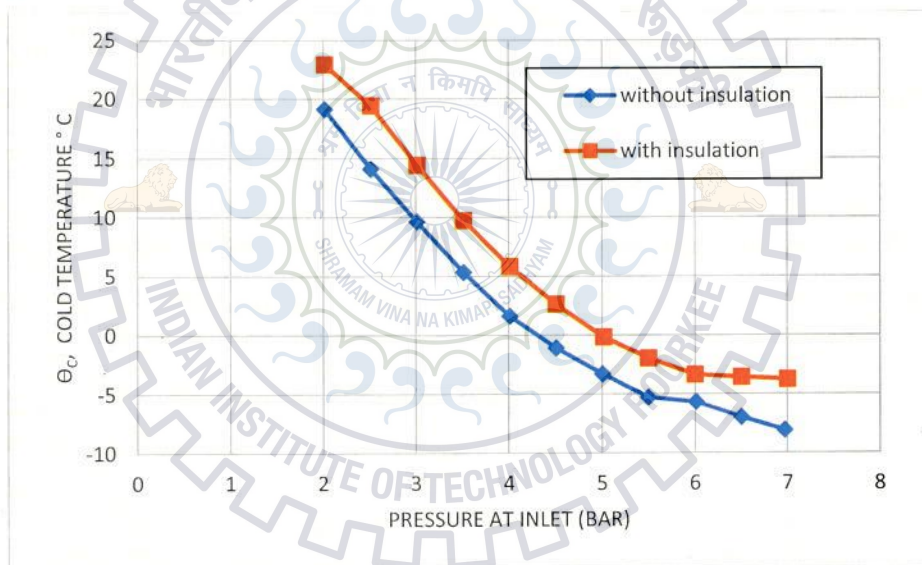


Fig.4.2.2: Variation of cold temperature with various inlet pressure.

Similarly Fig.4.2.3 shows the pattern of hot temperature with inlet pressure (absolute). As we know when inlet pressure of flow of air increase, nozzle create strong rotating flow inside tube. Large hot temperature depends upon the inlet pressure.

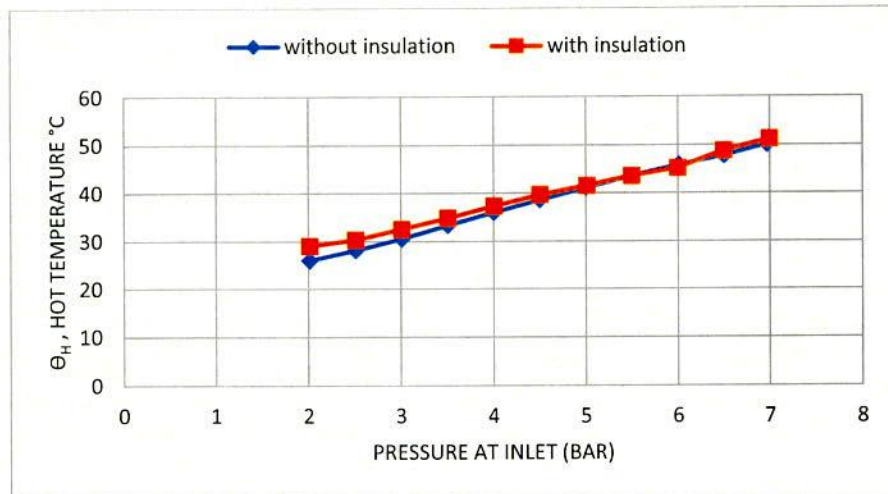


Fig.4.2.3: Variation of hot temperature with various inlet pressure.

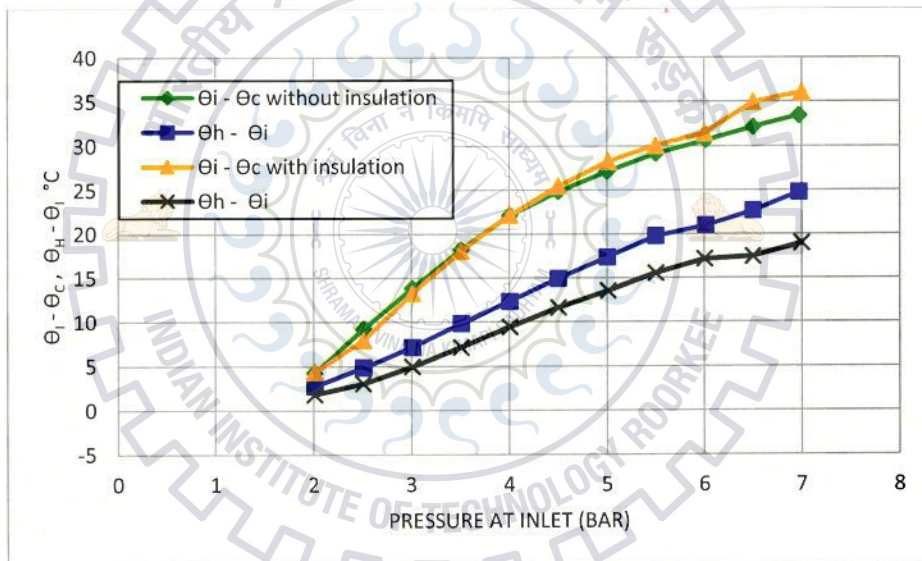


Fig.4.2.4: Variation of cold and hot temperature drop with various inlet pressure.

Fig 4.2.4 and Fig.4.2.5 show the variations of cold, hot temperature drop and relative humidity with the pressure in both cases of insulation and without insulation. Agrawal N. et al. [60] found cold temperature drop 23 °C at 5 bar. We found cold temperature drop at 5 bar is 27 °C.

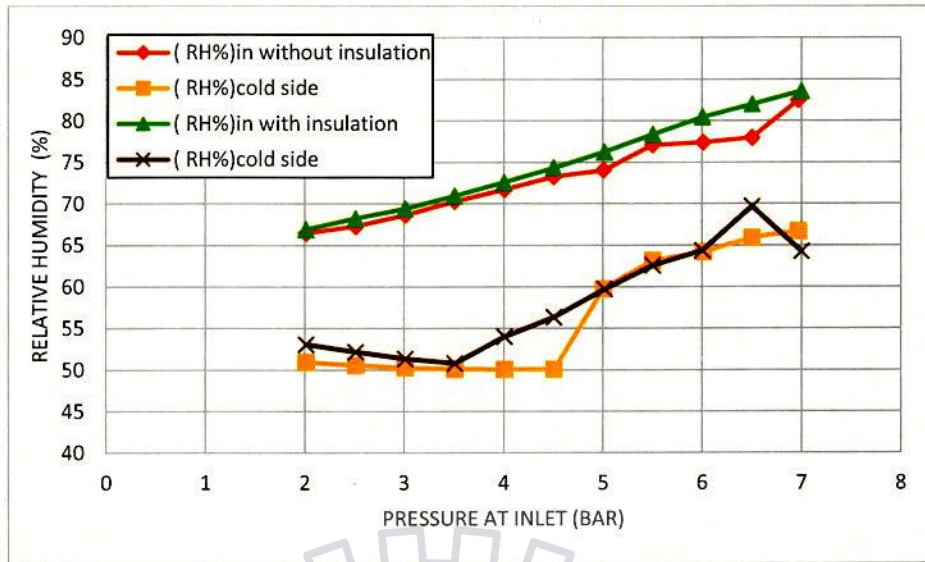


Fig.4.2.5: Variation of relative humidity with various inlet pressure.

4.3 Analysis of thermo physical properties at 50% Open control valve

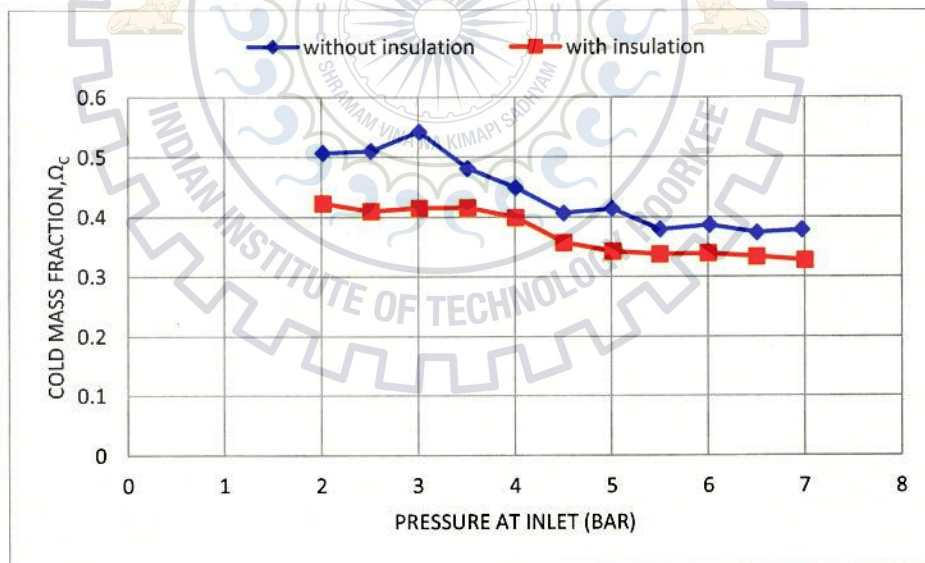


Fig.4.3.1: Variation of cold mass fraction Ω_c with various inlet pressure.

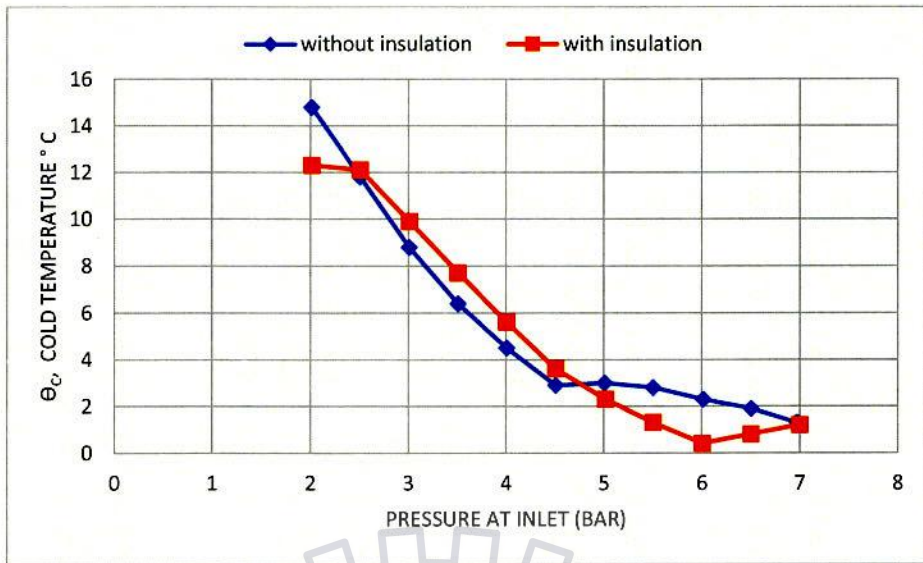


Fig.4.3.2: Variation of cold temperature with various inlet pressure.

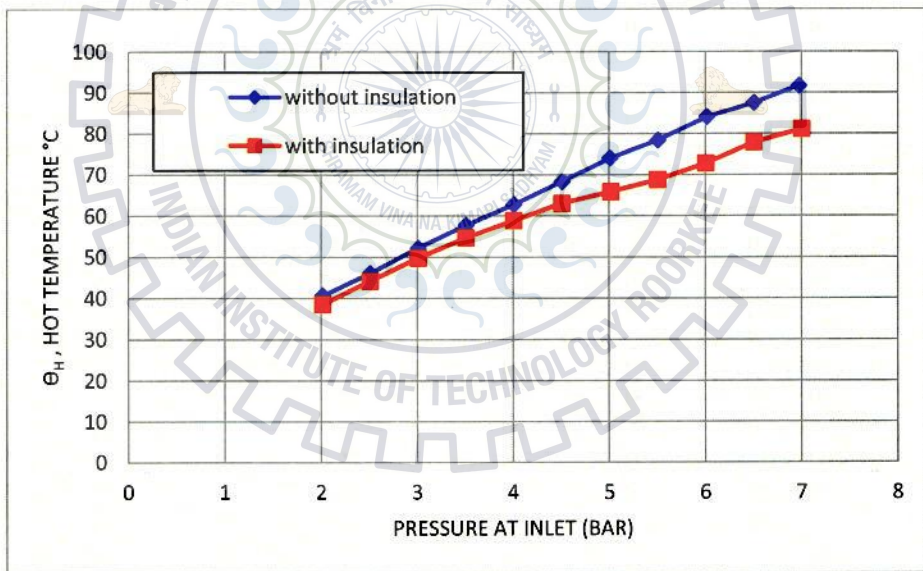


Fig.4.3.3: Variation of hot temperature with various inlet pressure.

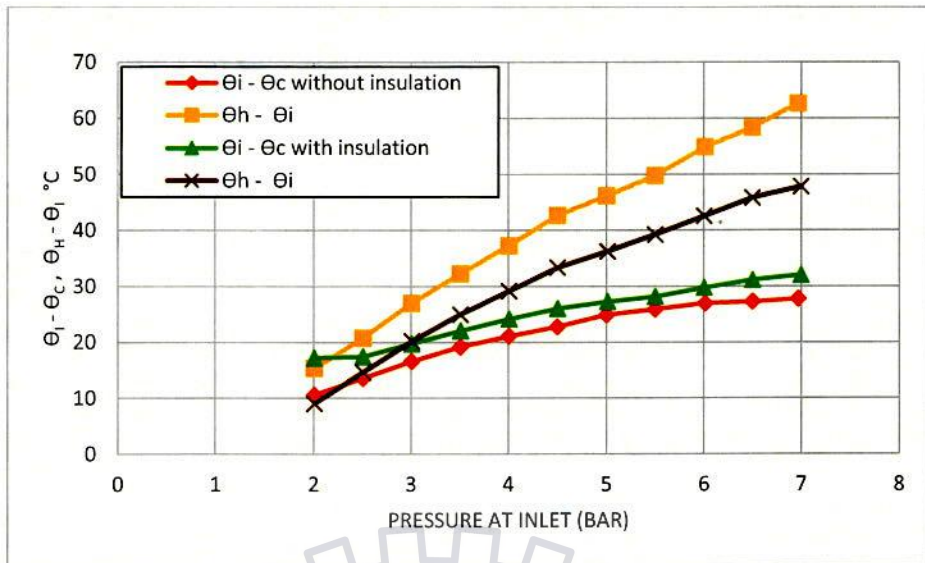


Fig.4.3.4: Variation of cold and hot temperature with various inlet pressure.

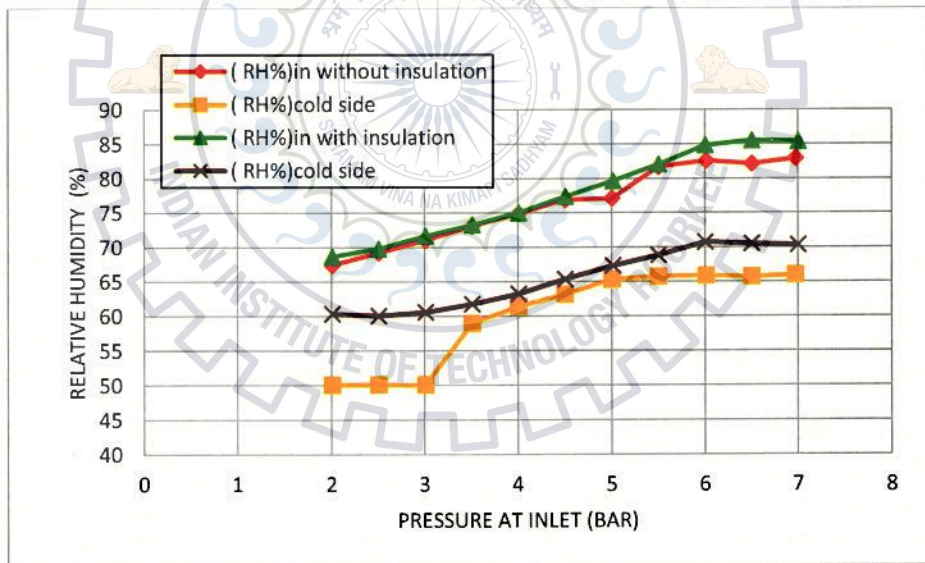


Fig.4.3.5: Relative humidity with various inlet pressure plot.

4.4 Analysis of thermo physical properties at fully close control valve

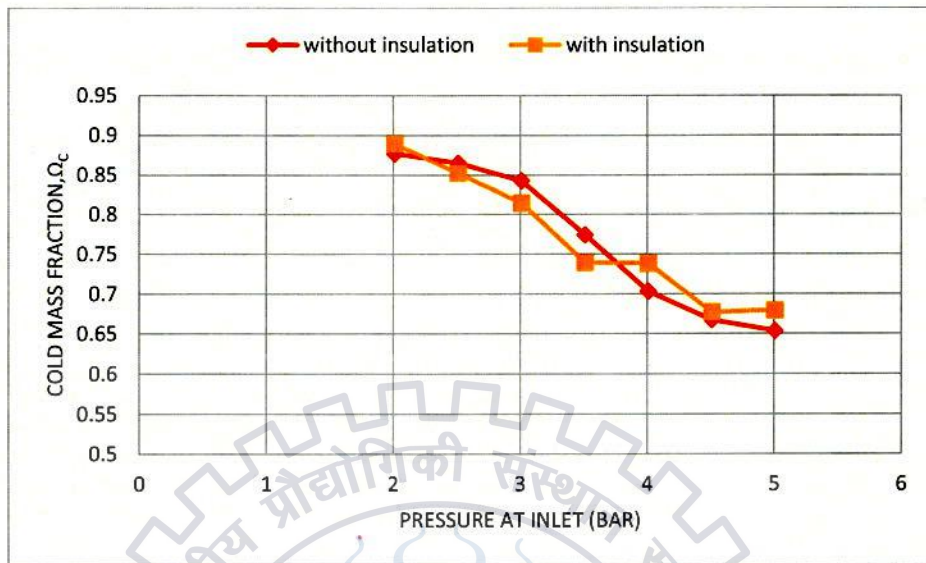


Fig.4.4.1: Variation of cold mass fraction Ω_c with various inlet pressure.

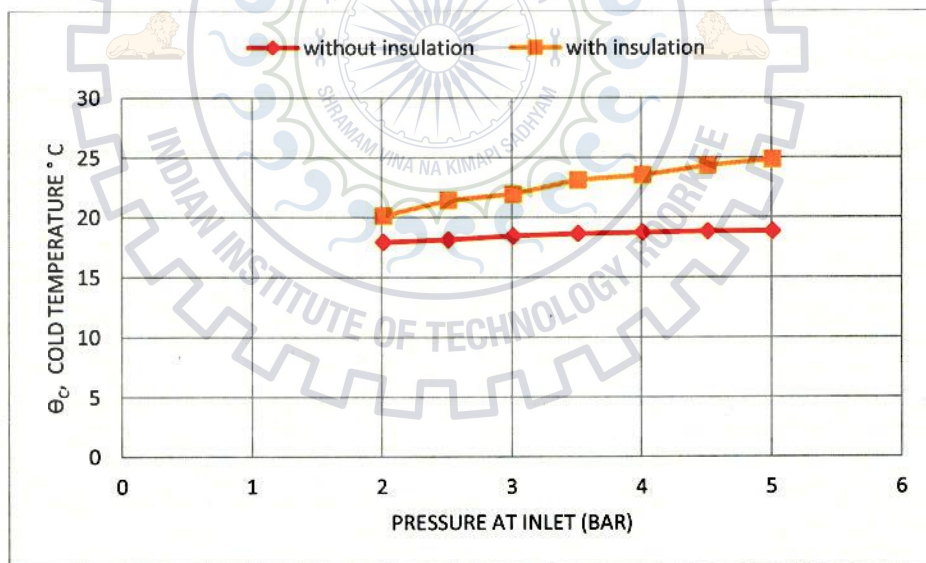


Fig.4.4.2: Variation of cold temperature with various inlet pressure.

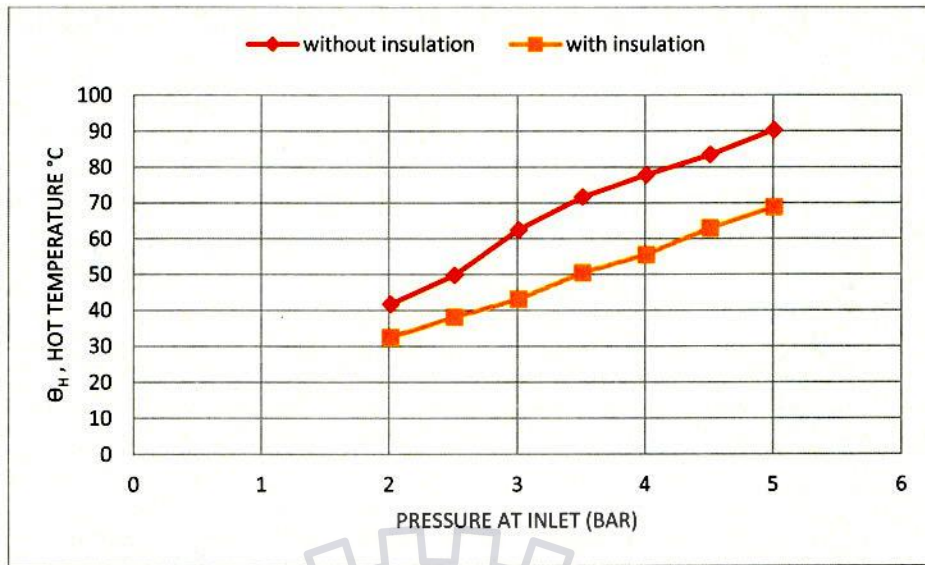


Fig.4.4.3: Variation of hot temperature with various inlet pressure.

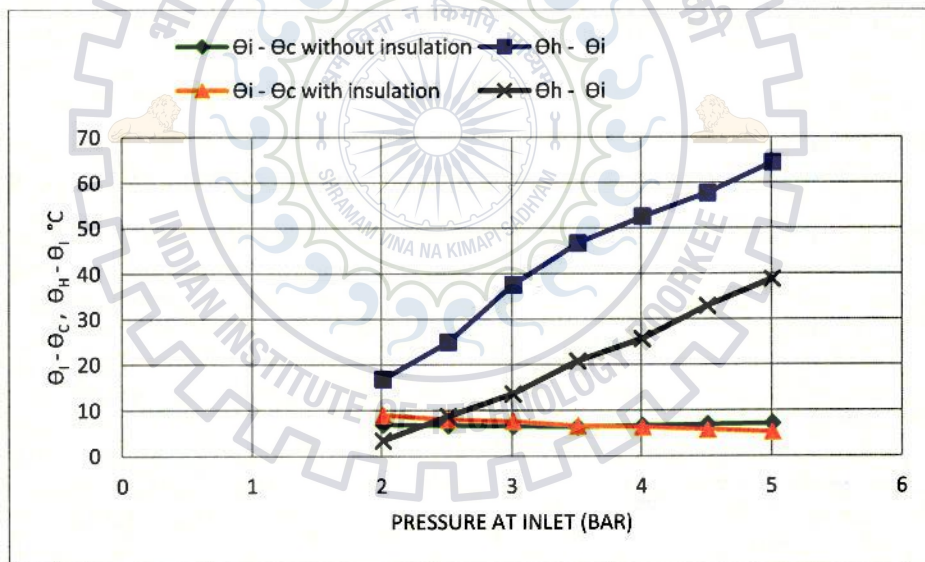


Fig.4.4.4: Variation of cold and hot temperature drop with various inlet pressure.

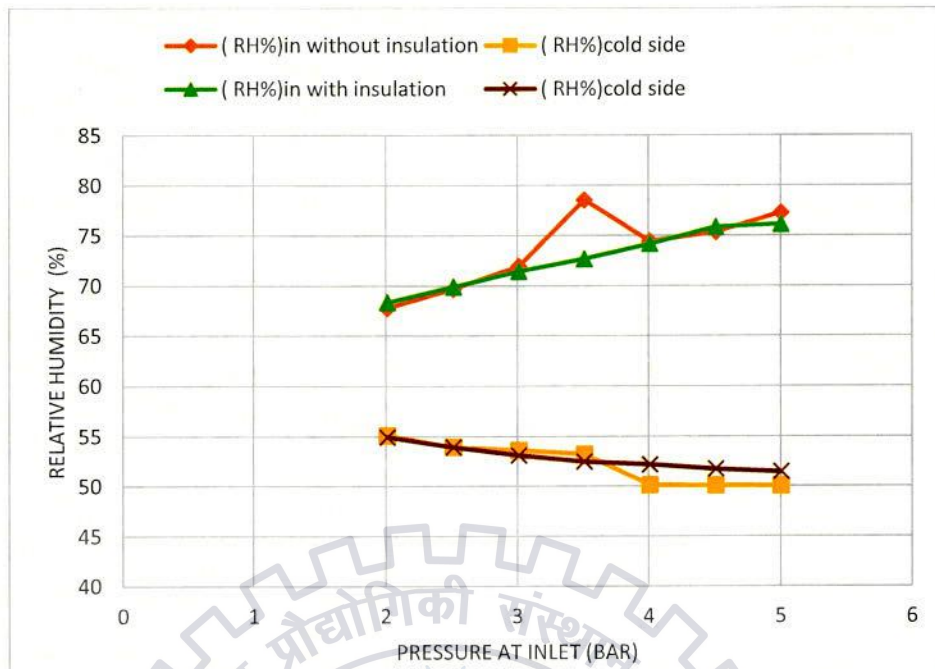


Fig.4.4.5: Variation of relative humidity with various inlet pressure.

Cold mass flow decreases when input pressure increase when fully close the hot end of vortex tube and results are shown in Fig.4.4.1. It is may be due to high pressure and closed position of valve, gas compress more, and eventually less formation of rotating flow. Cold temperature drop in both cases may show similar pattern shown in Fig.4.4.4. When valve are fully closed cold temperature increase, because of hot air at hot end return and mixed with centerline flow. Therefore cold air at orifice would be heated, same time temperature of hot air should be dropped, but this not happens because more air is compressed and stored at near the hot end and it increases the temperature of hot air. Graph of relative humidity is shown in Fig.4.4.5 with different pressures.

4.5 Cooling efficiency and Reynolds number analysis on vortex tube

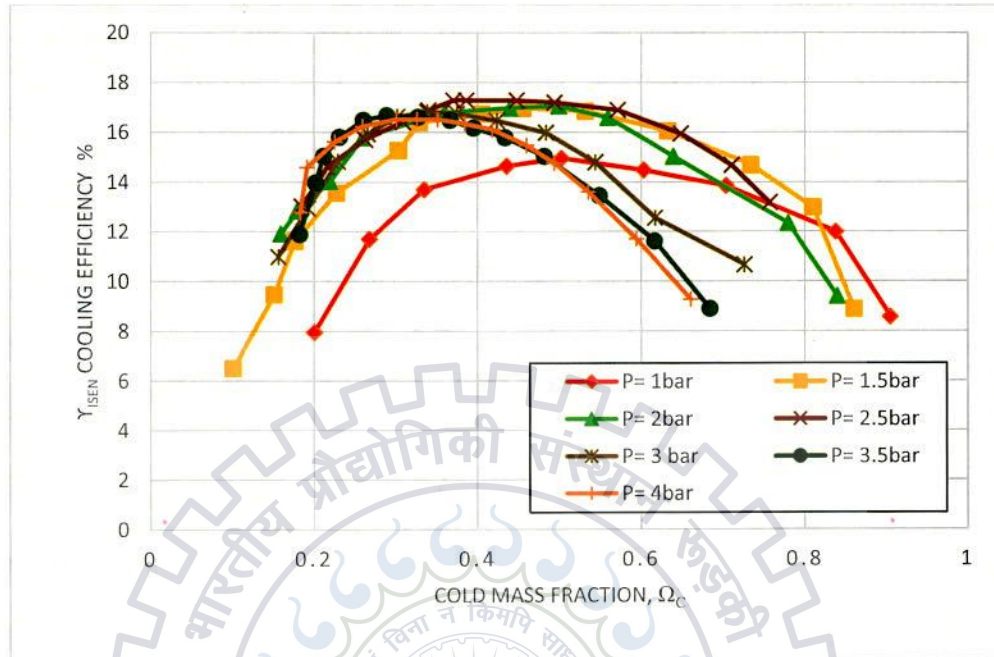


Fig.4.5.1: Variation of cooling efficiency with cold mass fraction at different inlet pressure without insulation on vortex tube.

From Fig.4.5.1 cooling efficiency increases with increase in cold mass fraction. At low inlet pressure we get optimum efficiency when mass fraction is in range of 0.35 to 0.45, after this cooling efficiency decreases. For high pressure we get better cooling efficiency at lower value of cold mass fraction. Mohammad S. V., and Nima N. [59] found maximum efficiency 19 % at 2 bar inlet pressure, cold mass fraction 20 %. We get maximum efficiency 17 % at cold mass fraction of 35 %~ 45 %.

Similar pattern is obtained when we use insulation on vortex tube as shown in Fig.4.5.2. Promvonge [52] get maximum efficiency 21 % at cold mass fraction 40 % using insulation on vortex tube with single nozzle entry. We get maximum efficiency 18 % at cold mass fraction in range of 38 % - 41 %.

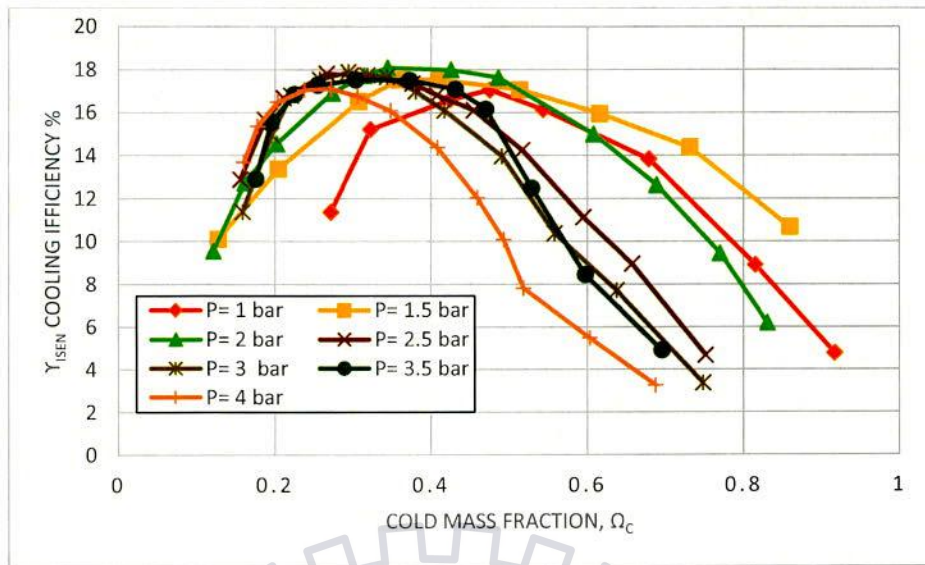


Fig.4.5.2: Variation of cooling efficiency with cold mass fraction at different inlet pressure with insulation on vortex tube.

Reynolds number at inlet of vortex tube does not much change with cold mass fraction at particular pressure. This is shown by Figure 4.5.3. Inlet Reynolds number lower at low pressure and higher for high pressure. Flow inside vortex is turbulent in nature, therefore Reynolds number play very important role to study performance on vortex tube.

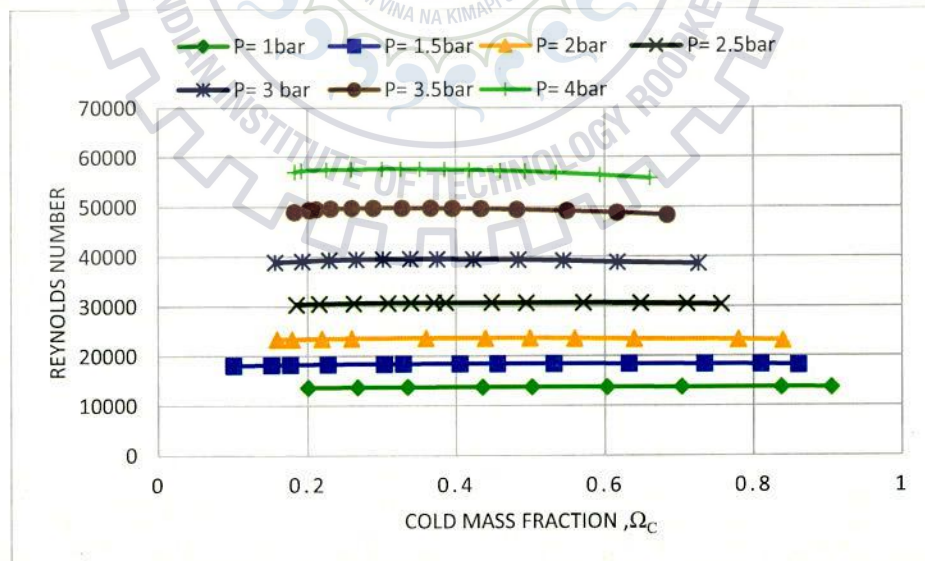


Fig.4.5.3: Variation of Reynolds number with cold mass fraction at different inlet pressure without insulation on vortex tube.

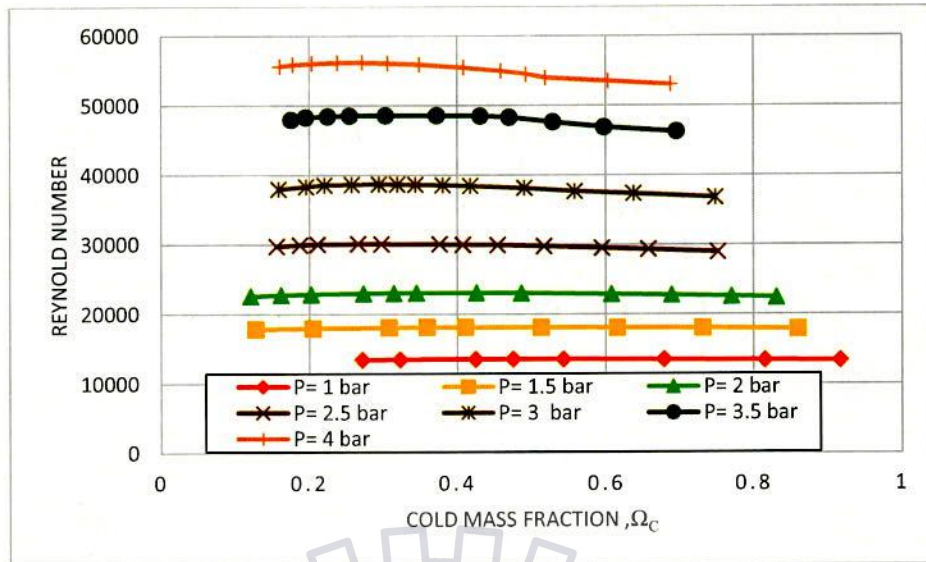


Fig.4.5.4: Variation of Reynolds number with cold mass fraction at different inlet pressure with insulation on vortex tube .

4.6 Reynolds number at different pressure when insulation use on vortex tube

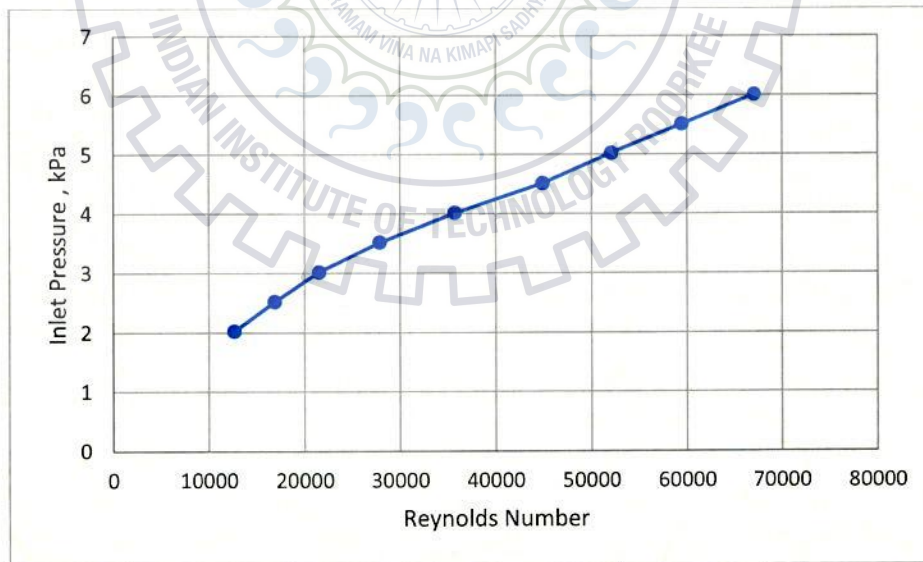


Fig.4.6.1: Input pressure function of Reynolds number.

From Fig.4.6.1 we observed Reynolds number increase with increase in input pressure. Hamoudi A. F. et.al. [58] found maximum Reynolds number of 8000 at pressure 0.8 bar. We get maximum Reynolds number of 68000 at pressure 6 bar.

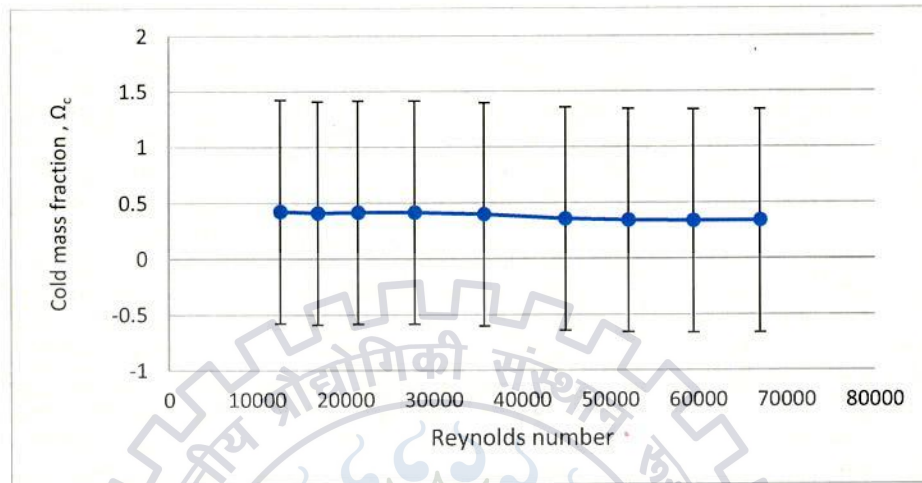


Fig.4.6.2: Variation of cold mass fraction with Reynolds number.

From Fig.4.6.2 cold mass fraction almost constant and decreases as increase in inlet Reynolds number. Hamoudi A. F. et al. [58] found optimum cold mass fraction of 0.65 at different values of inlet pressure. We get cold mass fraction almost near 0.50 at different values of inlet pressure with change in inlet Reynolds number

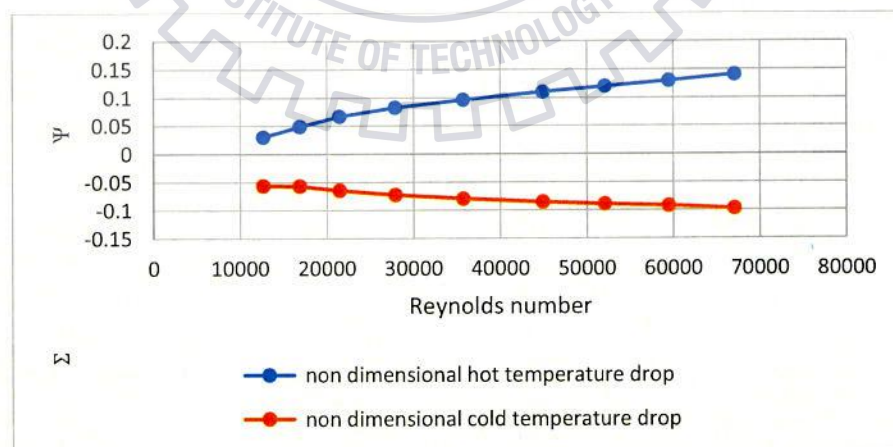


Fig.4.6.3: Variation of temperature drop with Reynolds number.

4.7 Reynolds number at different pressure without insulation on vortex tube

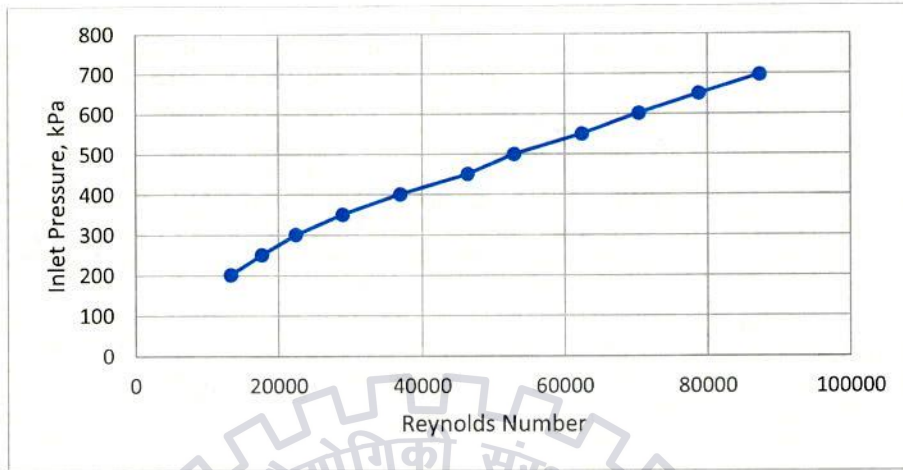


Fig.4.7.1: Input pressure function of Reynolds number.

From Fig.4.7.1 we observed Reynolds number increase with increase in input pressure. Hamoudi A. F. et.al. [58] found maximum Reynolds number of 8000 at pressure of 0.8 bar. We get maximum Reynolds number of 90000 at pressure of 700 kPa.

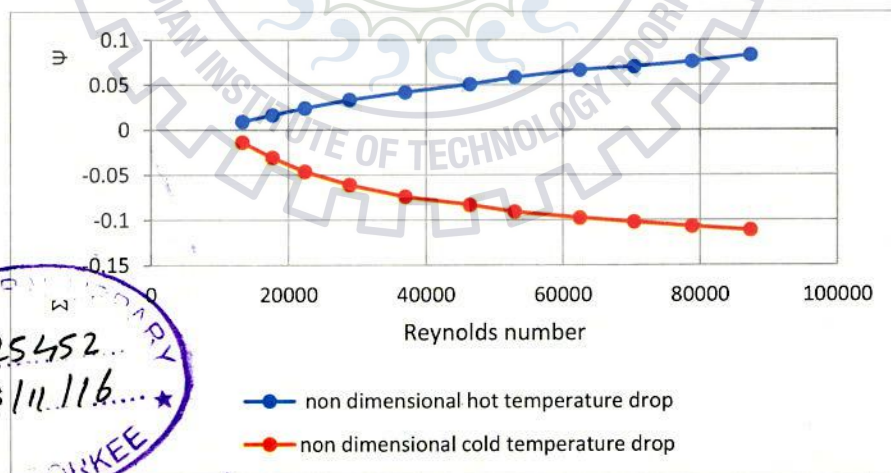


Fig.4.7.2: Variation of temperature drop with Reynolds number without insulation.



In figure 4.7.2 & Fig.4.6.3 non- dimensional cold temperature increase with increase in Reynolds number and non-dimensional temperature increase with increase in Reynolds number. Hamoudi A. F. et al. [58] found maximum value of non-dimensional hot temperature drop of 0.004 and non-dimensional cold temperature drop of -0.007 at low Reynolds number of 4000. We get maximum hot and cold non-dimensional temperature drop of 0.08 and -0.12 respectively at Reynolds number of 90000.

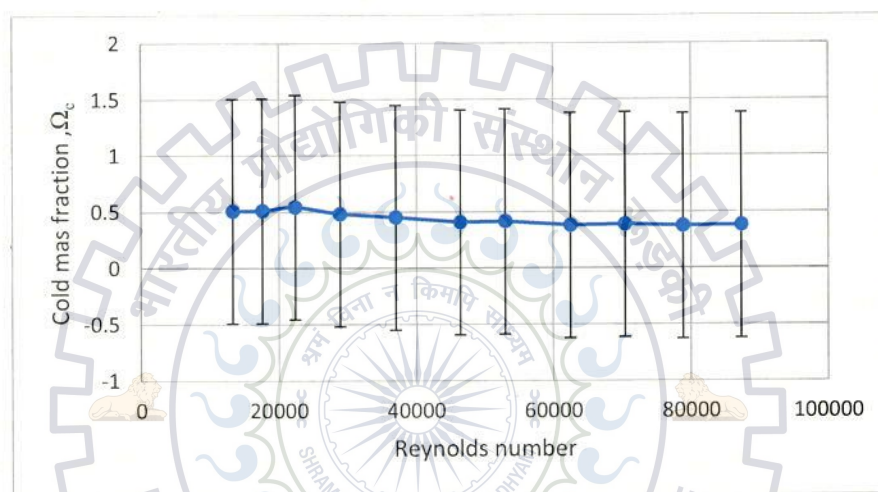


Fig.4.7.3: Variation of cold mass fraction with Reynolds number.

From Fig.4.7.3 cold mass fraction almost constant and decreases as increase in inlet Reynolds number. Hamoudi A. F. et al. [58] found optimum cold mass fraction of 0.65 at different value of inlet pressure. We get cold mass fraction almost near of 0.50 at different value of inlet pressure with change in inlet Reynolds number.

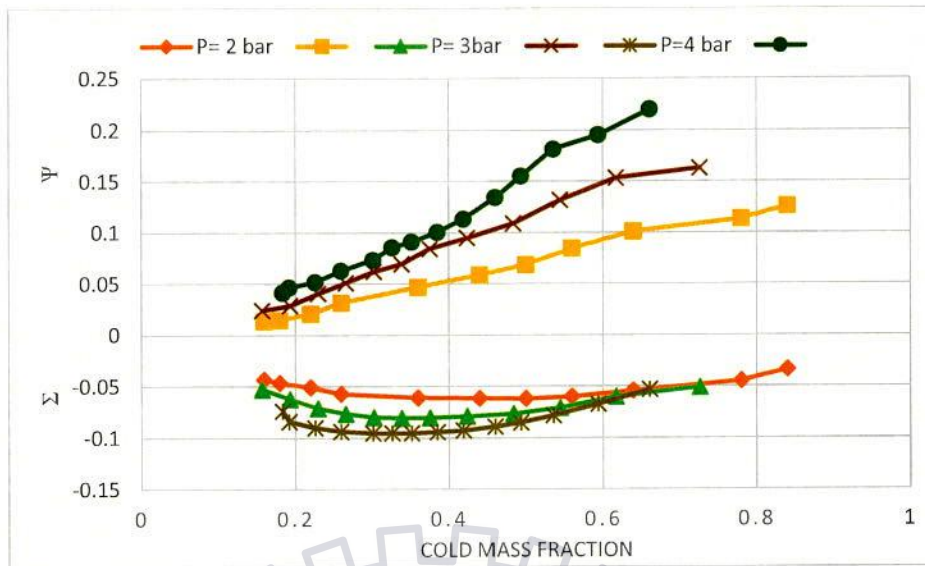


Fig.4.7.4: Variation of non-dimensional temperature drop with cold mass fraction (no insulation).

Increase in inlet pressure at inlet nozzle means increase in Reynolds number. It means at higher value of Reynolds number we have get more cold non-dimensional temperature it is shown in figure 4.7.1 and figure 4.7.2. From figure 4.7.4 non-dimensional temperature increases for value of cold mass fraction 0.25~ 0.35 at pressure 4 bar. For 2 and 3 bar pressure non-dimensional temperature less than pressure at 4 bar observe from figure 4.7.4. Similar is obtain in fig.4.7.5.

Hamoudi A. F. et al. [58] found maximum non-dimensional cold temperature drop of -0.015 at pressure 0.2 bar, of -0.025 at 0.3 bar and of -0.045 at 0.4 bar and maximum non-dimensional hot temperature drop almost 0.015 at pressure 0.2, 0.3 and 0.4 bar. We get maximum non-dimensional cold temperature drop of -0.06, -0.08 and -0.099 at pressure 2, 3 and 4 bar respectively. Non-dimensional hot temperature drop increases with increase in cold mass fraction.

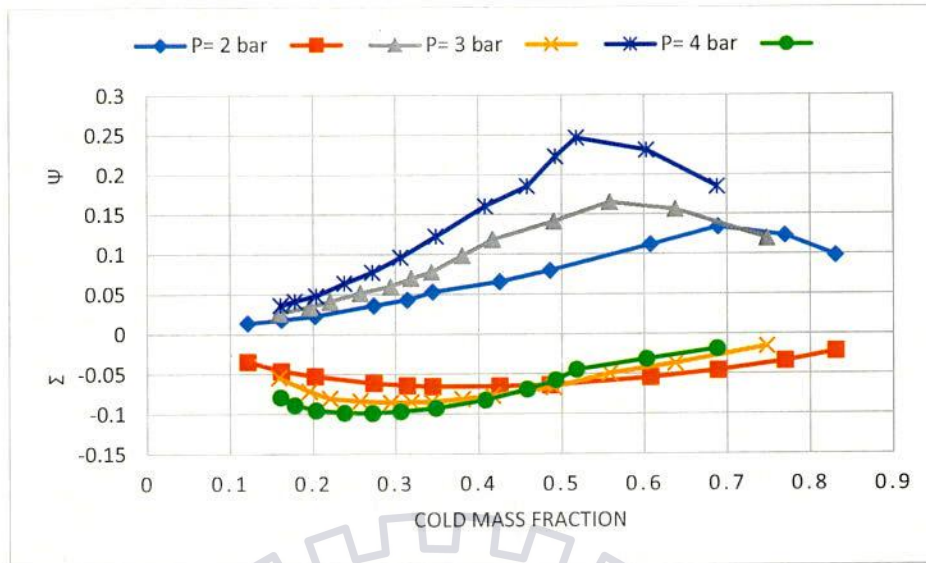


Fig.4.7.5: Variation of non-dimensional temperature drop with cold mass fraction (insulation on vortex tube).

From Fig.4.7.5 maximum non-dimensional cold temperature drop of -0.06, -0.08 and -0.1 at pressure 2, 3 and 4 bar respectively in cold mass fraction range of 0.25~0.30. Non-dimensional hot temperature drop 0.25, 0.15 and 0.12 at pressure 4, 3 and 2 bar respectively.

4.8 Coefficient of performance of Ranque-Hilsch vortex tube

In this section we investigate coefficient of performance with cold mass fraction and inlet pressure. Fig.4.8.1 and Fig.4.8.2 show the Variation of COP with cold mass fraction, it increases with increase in cold mass fraction then it became maximum with cold mass fraction in range Ω_c of 0.4 ~ 0.55, after it decreases with increase in cold mass fraction.

Jose Roberto S.M [62] found optimum COP =1 at inlet pressure 5 bar, cold mass fraction of 0.8. We found maximum COP of 0.1 at 1.5 bar inlet pressure, and COP of 0.06 at 4 bar inlet pressure.

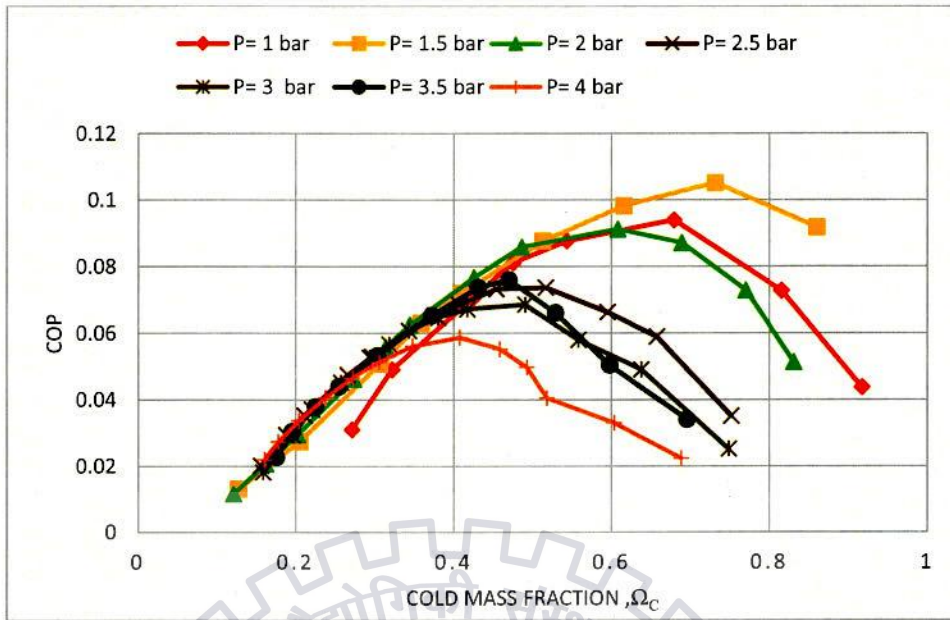


Fig.4.8.1: Variation of COP with cold mass fraction with insulation.

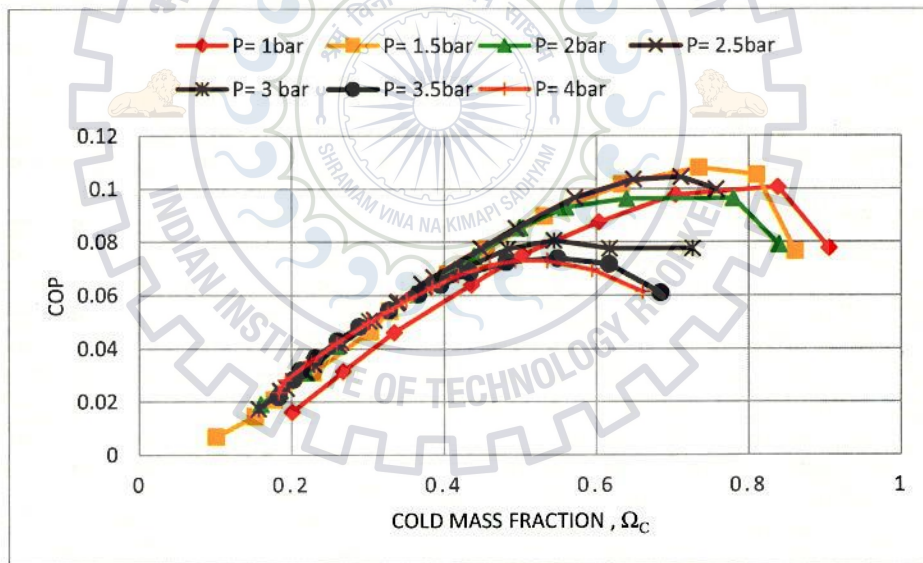


Fig.4.8.2: Variation of COP with cold mass fraction without insulation.

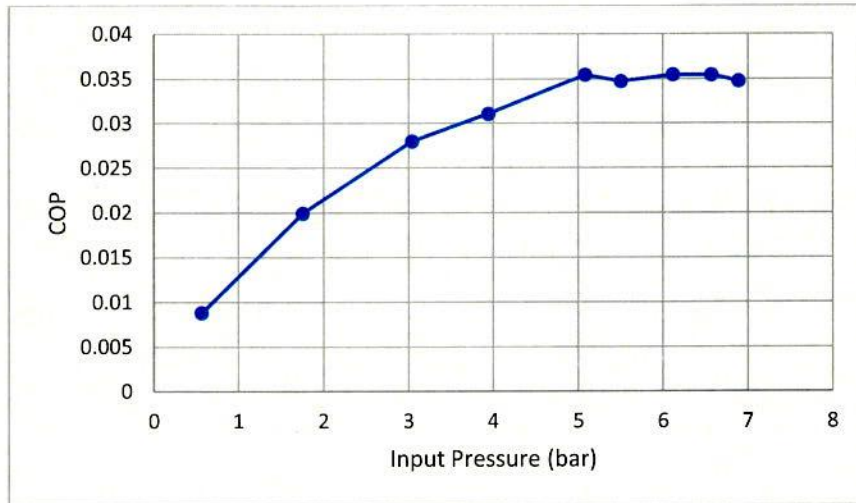


Fig.4.8.3: Variation of COP with inlet pressure (without insulation).

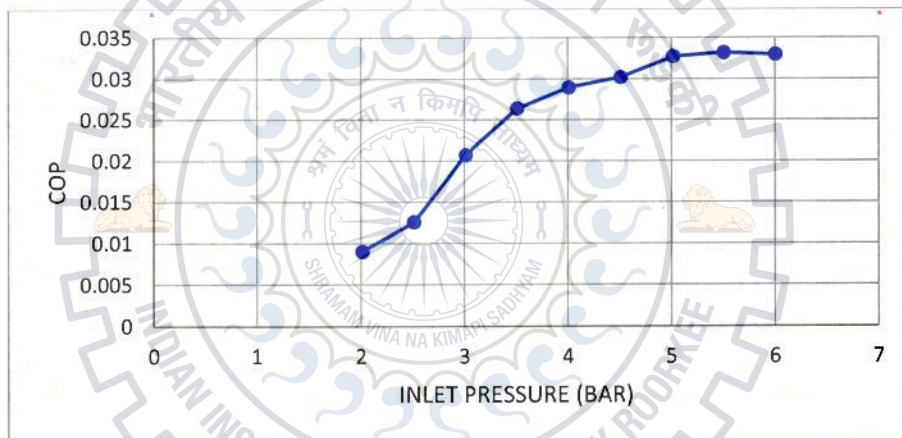


Fig.4.8.4: Variation of COP with inlet pressure (with insulation).

From Fig.4.8.3 and Fig.4.8.4 COP is very sensitive to inlet pressure up to pressure 5 bar, after this pressure COP does not much change. It is because of at high pressure more temperature separation occur, therefore we get more cold temperature. At very high pressure weak vortex motion generate within the vortex tube because there will be some flow restriction.

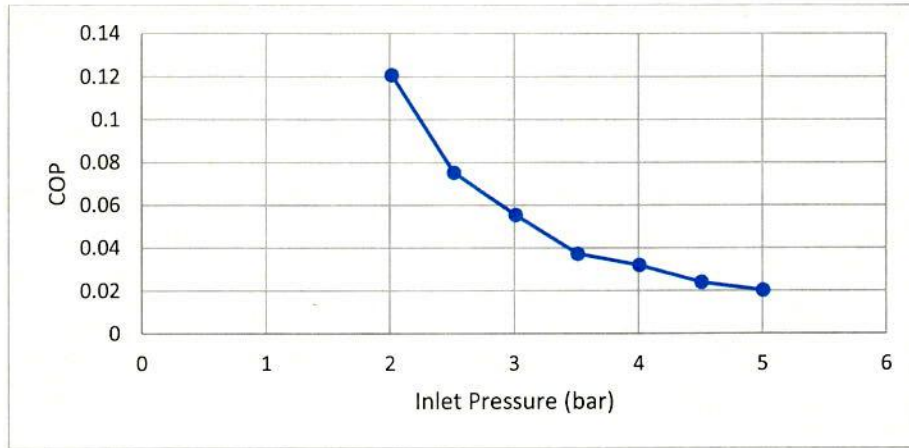


Fig.4.8.5: Variation of COP with inlet pressure (with insulation) at fully closed control valve.

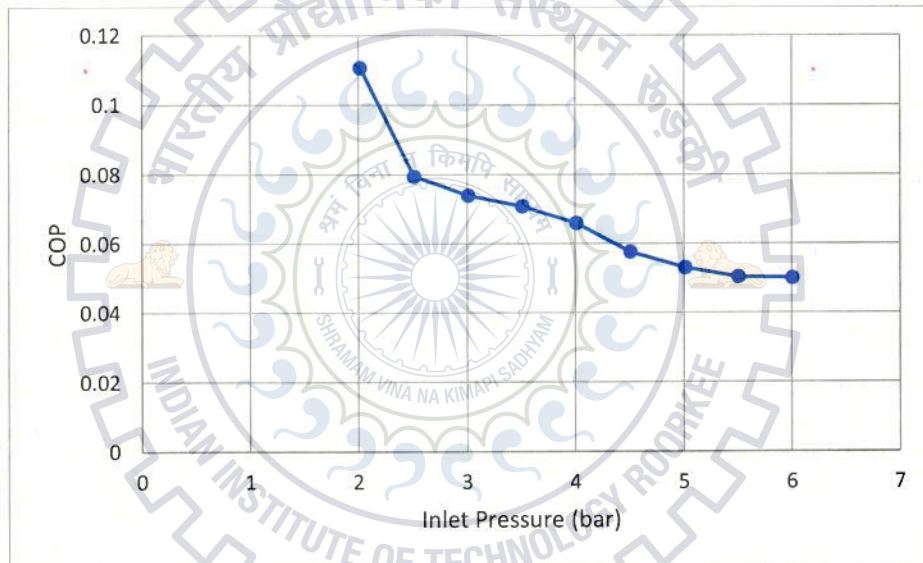


Fig.4.8.6: Variation of COP with inlet pressure (with insulation) at 50 % closed hot control valve.

Jose Roberto S.M [62] found similar type of Variation of COP with different inlet pressure. Its decreases with increases inlet pressure, later it become flat in nature at very high pressure.

Sudhakar Subudhi and Mihir Sen [63] found maximum COP of ~0.12 at cold mass fraction of 0.7. From Fig.4.8.1 and Fig.4.8.2 we get maximum value of COP of 0.12 at pressure of 1.5 bar, cold mass fraction of 0.7 in both cases i.e. with and without insulation on vortex tube.

CONCLUSION AND FUTURE SCOPE OF WORK

Thermal comfort is defined as condition to achieve reliable environmental temperature and humidity at which human being feel in comfort zone. It is done by combination of following processes: heating, cooling, and ventilation. We use Ranque- Hilsch vortex tube for thermal comfort in room size ($3\text{lx}3\text{bx}3\text{h}=37\text{ m}^3$). In this experimental study we presented and discussed how vortex tube parameter like cold mass fraction, pressure at inlet and input temperature affect on cold, hot temperature drop and relative humidity at exit of cold orifice.

From experiment, we found that cold temperature drop increases with increasing inlet pressure. It is due to the strong rotary motion of air created due to the high pressure air entering the radial nozzle. Due to this effect, we have got maximum temperature separation: $-4\text{ }^\circ\text{C}$ at cold end and $95\text{ }^\circ\text{C}$ at hot end.

Cold temperature decreases with the increase in cold mass fraction, later increases with the increase in mass fraction. We get cold temperature due to expansion of air and hot temperature due to adiabatic compression and it is also due to viscous shear between fluid layers, momentum transfer and strong vortex flow generation.

Air enters the vortex tube at high humidity and it is dehumidified at the exit of cold orifice. Humidity also depends upon the value of inlet pressure and cold mass fraction. It is experimentally found that humidity first increases with the increase in cold mass fraction then decreases with the increase in mass fraction closer to one. Humidity depends upon different parameters such as velocity, air temperature and environment. Humidity also changes with the pressure; it increases as pressure increases.

Humidity at $P=1\text{ bar}$ have almost linear variation with cold mass fraction. At high pressure, there is large change in humidity. Air dehumidification increases with the increase in cold temperature drop. There is formation of water droplet at cold end.

Phenomenon of energy/ temperature separation is still unclear due to complex nature of flow inside the tube. Therefore it needs some excellent techniques like particle image velocimetry, particle tracking velocimetry to identify the flow structures.

It needs more investigations on multi-circulation to study how energy transfer from cold fluid to hot fluid.

From experimental results, it is found that cooling efficiency is less. Therefore it should be investigated to improve this efficiency.



APPENDIX

1.1 Calculation of cooling capacity for room size (3LX3BX3H = 27 m³)

Outdoor condition 35 DBT, 70 % RH,

Indoor condition 25 DBT, 50 % RH

Room size (3LX3BX3H = 27m³)

Number of person = 3

Using formula for breathing zone outdoor airflow

$$V_{bz} = R_p P_z + R_a A_z$$

From ASHRAE

$$R_p = 5 \text{ cfm / person}, P_z = 3, R_a = 0.06 \text{ cfm/ft}^2 \text{ (for office)}, A_z = 96.875194 \text{ ft}^2$$

$$V_{bz} = 5 \cdot 3 + 0.06 \cdot 96.875194$$

$$= 20.8125 \text{ cfm}$$

$$= 35.38125 \text{ m}^3/\text{h}$$

v_1 (= 0.9095 m³/kg specific volume at outdoor condition) from psychrometric chart

$$\text{Mass of air } \dot{m}_a = V_{bz} / v_1$$

$$= 38.90186 \text{ kg/h}$$

$$\text{Capacity of cooling} = \dot{m}_a (h_1 - h_2) \text{ kJ/h}$$

$$= 38.90186(98-50) \text{ kJ/h}$$

$$= 1867.289 \text{ kJ/h}$$

$$= 0.51869 \text{ kJ/s}$$

$$= 0.14819 \text{ TR}$$

Amount of water removed in dehumidification process

$$\dot{m}_w = \dot{m}_a (\omega_1 - \omega_2) \text{ g/h}$$

$$= 38.90186(25.2-10) \cdot 10^{-3} \text{ kg/h}$$

$$= 0.59130 \text{ kg/h}$$

1.2 Calibration

1.2.1 Pressure transducer

Electronic pressure transducer of range 1 - 16 bar and its output are 4 mA to 20mA as shown in Fig.5.1. To minimize error in experimental reading calibration is performed on the dead weight tester along DAQ system (Yokogawa) to make correct value of reading. A dead weight tester is device in which pressure is to apply fluid to check the accuracy of pressure gauge or pressure transducer. Dead weight tester is standard calibration unit with piston, cylinder on which load is placed to make equilibrium with an applied pressure. Formula on which dead weight tester is design based on the $P=F/A$. A graph is plotted between the value from DAQ system on X- axis and from calibration value on Y- axis. A correlation is found from graph using regression analysis.

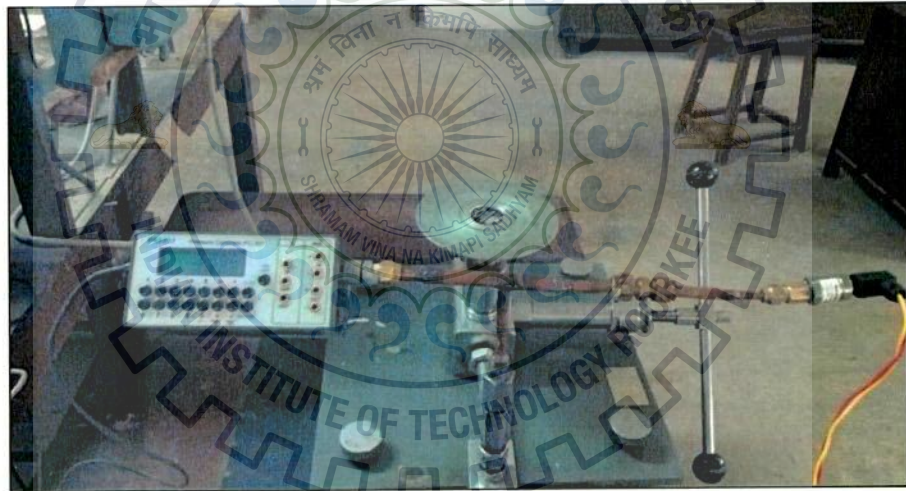


Fig.6.1: Dead weight tester with pressure transducer.

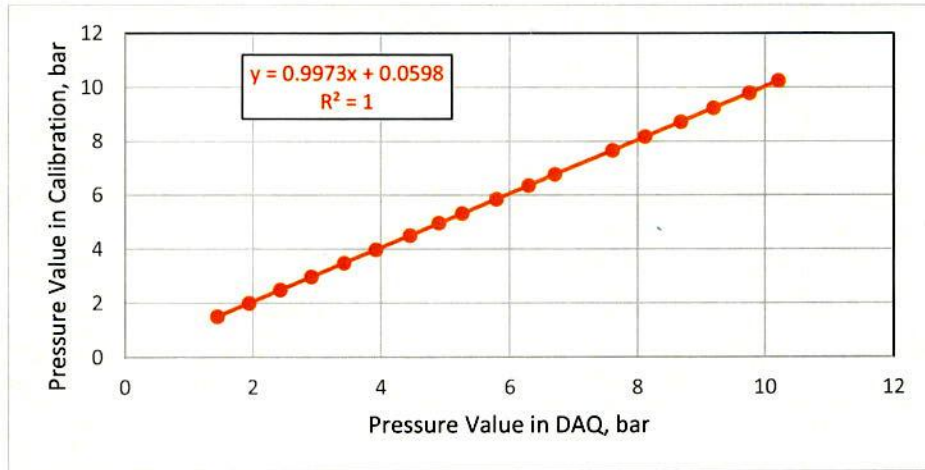


Fig.6.2: Showing calibration between pressure value in DAQ and pressure value in calibration system for transducer range (0-16 bar).

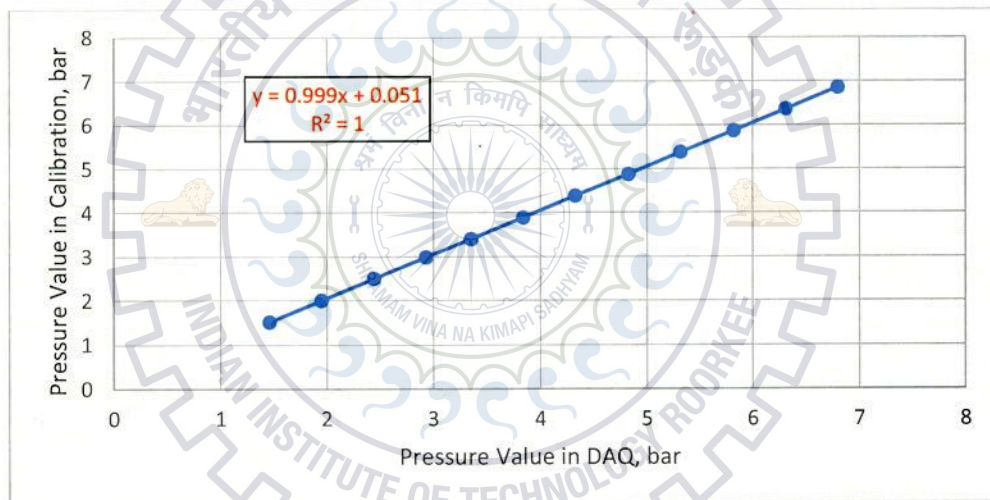


Fig.6.3: Showing calibration between pressure value in DAQ and pressure value in calibration system for transducer range (0-10bar).

1.2.2 Temperature calibration

First we make thermocouples based on the see-beck effect. See-beck is conversion of temperature difference to electricity. It is discover by see-beck. Compass needle would be deflected in when a closed loop is form by two different metal joining at two place with temperature difference between two junctions. This is because metal response temperature difference in different way creating current loop and magnetic field.

$$j = \sigma(-\Delta V + E_{emf})$$

$$-\Delta V = S\Delta T$$

S is seebeck coefficient and function of temperature difference.

When steady state reach value of current density zero. This become simple equation. Thermocouples are calibrate using presys T-25N calibrator. A graph is plotted shown in Fig.5.1 between temperature value from DAQ and temperature from calibration system. X-axis represent the value from DAQ and Y- axis represent the value from calibrator unit. A linear correlation is found.

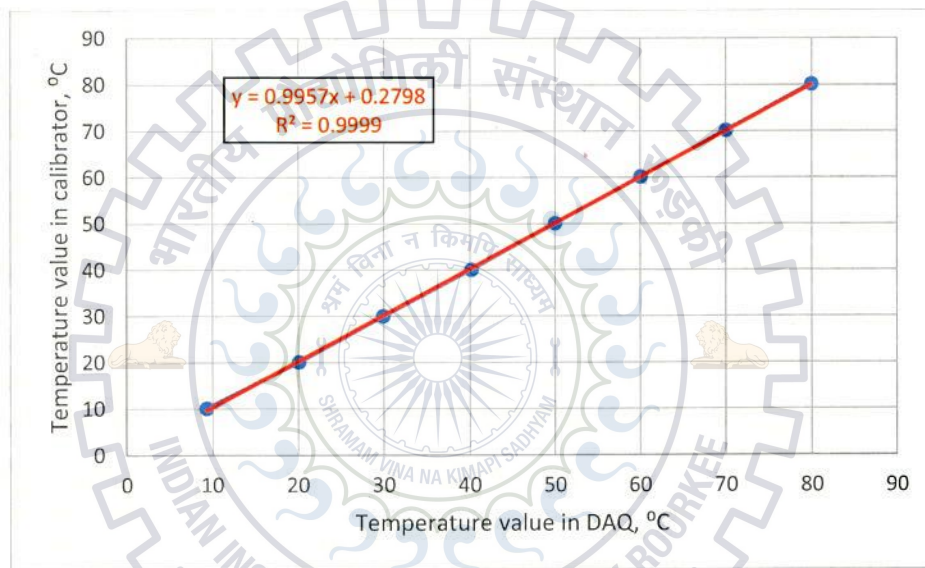


Fig.6.4: Calibration data with correlation for temperature.

1.2.3 Humidity sensor calibration

We use total two relative humidity sensor in this experiment, one at inlet of vortex tube and other at cold exit. Sensor name 2 are use at inlet and sensor name 1 at exit of vortex tube. To minimize the errors in results need to calibrate instrument which are used in experiment. A graph is plotted as shown in Fig.6.5 and Fig.6.6 between value from sensor on X- axis and value from digital Hygrometer on Y- axis.

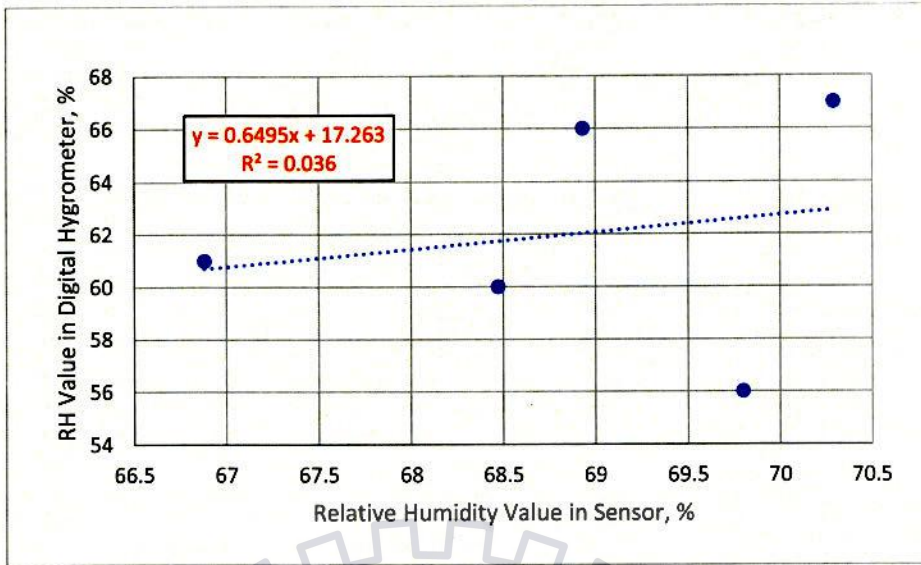


Fig.6.5: Calibration data with correlation for sensor 2.

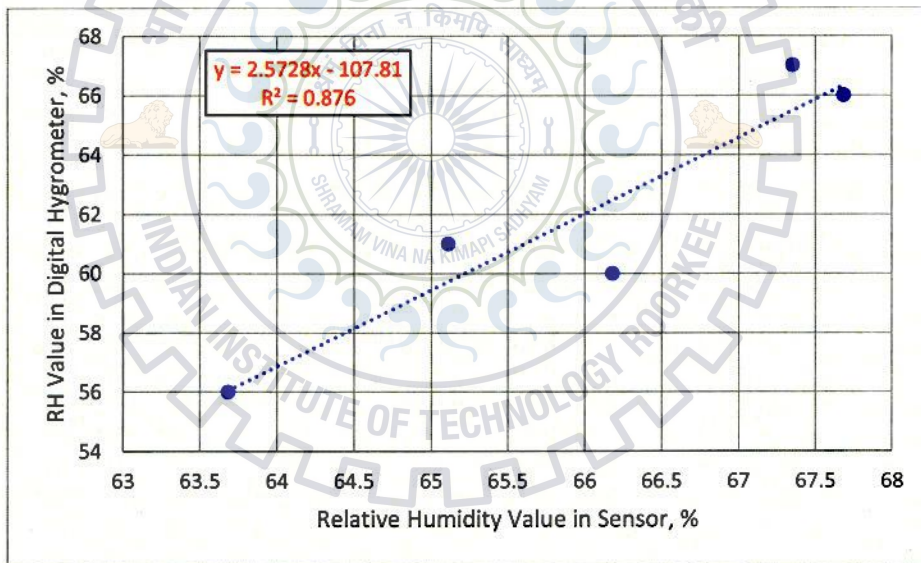


Fig.6.6: Calibration data with correlation for sensor 1.

1.2.4 Rotameter calibration

To calibrate variable area rotameter we use oxygen filled cylinder and weighing machine (analog type). First we measure the weight of oxygen filled cylinder then allow to escape the gas from cylinder and again weight the cylinder for every 1 kg of oxygen gas escape from cylinder. Time taken to escape every 1 kg of gas is measure by using stop watch. We repeat this for every step of measurement. Pressure regulator is also used to make pressure constant at exit of oxygen cylinder. We make some mathematical analytical to equalize oxygen cylinder in to air cylinder.

Total weight of oxygen cylinder = 78 kg

Weight of oxygen cylinder = 7 kg

Amount of oxygen gas by weight is 23.20 kg in 100 kg of air.

$$1 \text{ kg of O}_2 = \frac{100}{23.20} \text{ kg of air}$$

Therefore in

$$7 \text{ kg of O}_2 = 30.172 \text{ kg of air}$$

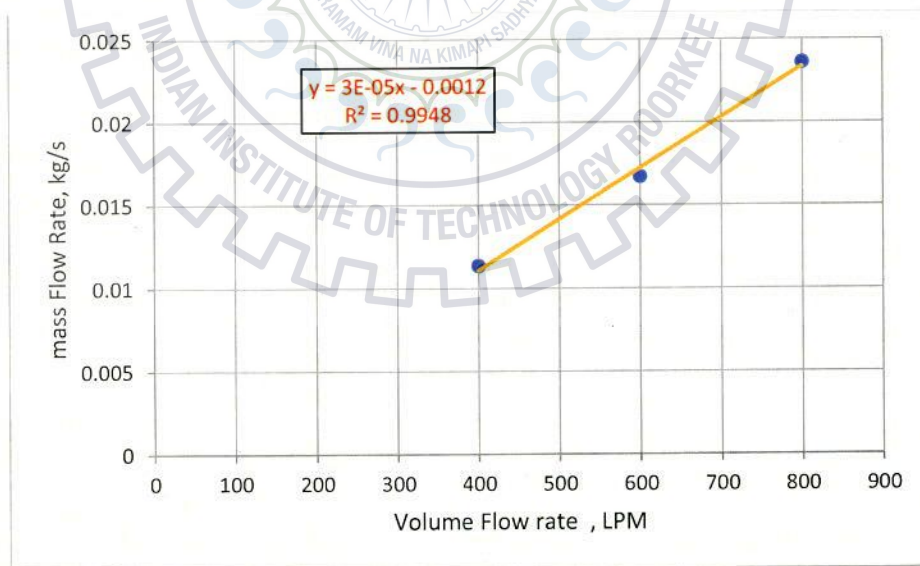


Fig.6.7: Calibration data with correlation for rotameter range (80-800) LPM.

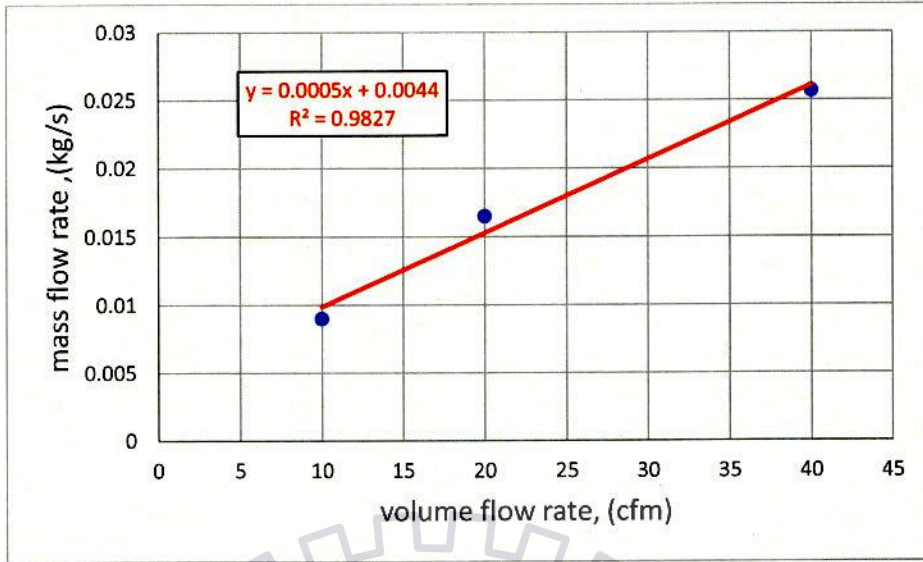


Fig.6.8: Calibration data with correlation for rotameter range (10-100) CFM.

1.2.5 Dynamic viscosity

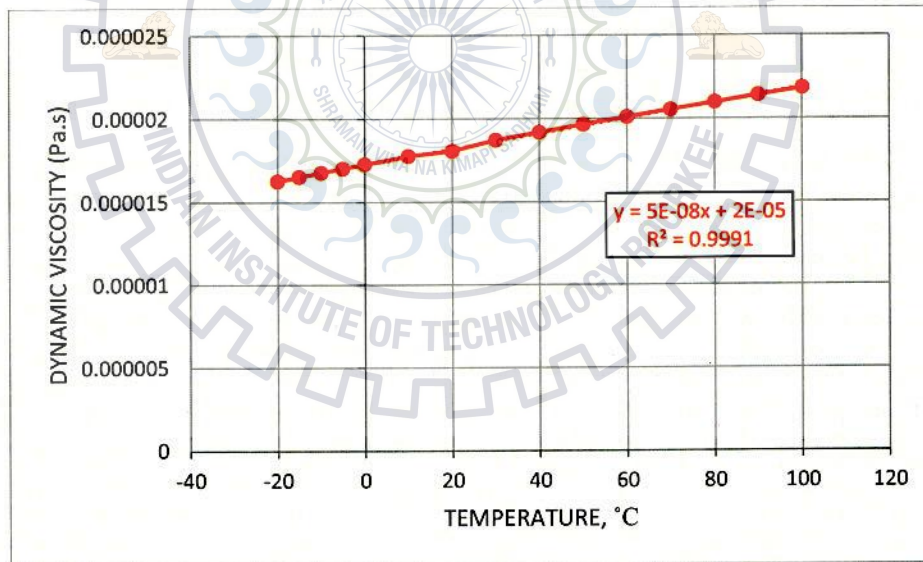


Fig.6.9: Variation of dynamic viscosity with temperature, and correlation equation.

REFERENCES

1. Ranque G.J., "Experiments on expansion in a vortex with simultaneous exhaust of hot air and cold air", *J. Phys. Radium (Paris)*, (1933), Vol. 4, pp. 112.
2. Ranque G.J., "Method and apparatus for obtaining from a fluid under pressure two outputs of fluid at different temperatures", US patent No.1:952, (1934), pp.281.
3. Hilsch R., "The use of expansion of gases in a centrifugal field as a cooling process", *Rev Sci Instrum*, (1947), Vol. 18 (2), pp. 108–113.
4. Scheper G.W., "The vortex tube, internal flow data and a heat transfer theory", *J ASRE Refrig Eng.* (1951), Vol. 59 pp. 985–990.
5. Martynovskii V.S., Alekseev V.P., "Investigation of the vortex thermal separation effect for gases and vapors", *Sov Phys-Tech Phys*, (1956), Vol. 1, pp. 2233–2243.
6. Dobratz B.M., "Vortex tubes, a bibliography", Lawrence Radiation Laboratory, (1964) UCRL-7829., pp.742-752.
7. Curley W., McGree Jr. R., "Bibliography of vortex tubes", *Refrig Eng.*, (1951), Vol. 59 (2), pp. 191–203.
8. Kalvinskis L., "Vortex tubes (an extension of Wesley's bibliography)", Jet Propulsion Laboratory, California Inst of Technology Literature Search, (1956), Vol. 2, pp.56.
9. Riu K., Kim J., Choi I.S., "Experimental investigation on dust separation characteristics of a vortex tube", *Trans JSME Ser B: Therm. Fluid Mech.*, (2004), Vol. 47 (1), pp. 29–36.
10. Bruno T.J., "Applications of the vortex tube in chemical analysis Part I introductory principle", *Am Lab*, (1993), Vol. 25, pp. 15–20.
11. Ahlborn B., Camirte J., Kellar J.U., "Low pressure vortex tube", *J Phys D appl. Phys*, (1996), Vol. 29, pp. 1469-1472.
12. Colgate S.A., Buchler J.R., "Coherent transport of angular momentum-the Ranque–Hilsch tube a paradigm, astrophysical turbulence and convection", *Ann NY Acad Sci*, (2000), Vol. 898, pp. 105–112.
13. Xue Y., Arjomandi M., Kelso R., "Experimental study of the thermal separation in a vortex tube", *Exp. Therm. Fluid Sci.*, (2013), Vol. 46, pp. 175-182.
14. Eiamsa-ard R., Promvong P., "Review of Ranque–Hilsch effects in vortex tubes, renewable Tubes", *Renewable and Sustainable Energy Reviews* (2012), Vol. 12 (7), pp. 1822–1842.

15. Ahlborn B., Keller J.U., Staudt R., "Limits of temperature separation in a vortex tube", *J Phys D: Appl. Phys.*, (1994), Vol. 27, pp. 480.
16. Ahlborn B., Gordon J.M., "The vortex tube as a classic thermodynamic refrigeration cycle", *J Appl. Phys* (2009), Vol. 88 (6), pp. 3645.
17. Gutsol A.F., "The Ranque effect", *Physics-Uspkhi*, (1997), Vol. 40 (6), pp. 639.
18. Lewins J., Bejan A., "Vortex tube optimization theory", *Energy*, (1999), Vol. 24, pp. 931.
19. Xue Y., Arjomandi M., Kelso R., "Visualization of the flow structure in a vortex tube", *Experimental Thermal and Fluid Science*, (2011), Vol. 35, pp. 1514–1521.
20. Takahama H., "Studies on vortex tubes", *Bulletin of JSME*, (1965), Vol. 8, pp. 433–440.
21. Ahlborn B., Groves S., "Secondary flow in a vortex tube", *Fluid Dynamics Research*, (1997), Vol. 21, pp. 73–86.
22. Gao C.M., Bosschaart K.J., Zeegers J.C.H., De Waele A.T.A.M., "Experimental study on a simple Ranque-Hilsch vortex tube", *Cryogenics*, (2005), Vol. 45, pp. 173–183.
23. Dincer K., Yilmaz Y., Berber A., Baskaya S., "Experimental investigation of performance of hot cascade type Ranque-Hilsch vortex tube and exergy analysis", *International Journal of Refrigeration*, (2011), Vol. 34, pp. 1117–1124.
24. Dincer K., Avci A., Baskaya B., Berber A., "Experimental investigation and exergy analysis of the performance of a counter flow Ranque-Hilsch vortex tube with regard to nozzle cross-section areas", *International Journal of Refrigeration*, (2010), Vol. 33, pp. 954–962.
25. Aljuwayhel N.F., Nellis G.F., Klein S.A., "Parametric and internal study of the vortex tube using a CFD model", *International Journal of Refrigeration*, (2005), Vol. 28, pp. 442–450.
26. Behera U., Paul P.J., Dinesh K., Jacob S., "Numerical investigations on flow behavior and energy separation in Ranque-Hilsch vortex tube", *International Journal of Heat and Mass Transfer*, (2008), Vol. 51, pp. 6077–6089.
27. Eiamsa-ard S., Promvong P., "Numerical simulation of flow field and temperature separation in a vortex tube", *International Communications in Heat and Mass Transfer*, (2008), Vol. 35 (8), pp. 937–947.
28. Eiamsa-ard S., Promvong P., "Numerical investigation of the thermal separation in a Ranque-Hilsch vortex tube", *International Journal of Heat and Mass Transfer*, (2007), Vol. 50 (5–6), pp. 821–832.

29. Eiamsa-ard S., Promvong P., "Numerical investigations of compressible flow and energy separation in a counter-flow vortex tube", *International Journal of Fluid Mechanics Research*, (2007), Vol. 34 (4), pp. 308–331.
30. Simoes-Moreira J.R., "An air-standard cycle and a thermodynamic perspective on operational limits of Ranque–Hilsch or vortex tubes", *Int J Refrig.*, (2010), Vol. 33 (4), pp. 765–773.
31. Ramakrishna P.A., Ramakrishna M., Manimaran R., "Experimental investigation of temperature separation in a counter-flow vortex tube". *J Heat Transfer*, (2014), 136Art. No. 082801.
32. Williams A., "Cooling of methane with vortex tubes", *J. Mech. Eng. Sci.*, (1971), Vol. 13 (6), pp.369-375.
33. Collins R.L., Lovelace R.B., "Experimental study of two-phase propane expanded through the Ranque-Hilsch tube", *J. Heat Transfer*, (1979), Vol. 101, pp. 300-305.
34. Balmer R.T., "Pressure driven Ranque Hilsch temperature separation in liquids", *J. Fluid Eng.*, (1988), Vol. 10, pp. 161-164.
35. Jin H., Ji G., "Experimental research on gas liquid two-phase vortex tube characteristics", *Cryogenics*, (1995), Vol. 5, pp. 22-26.
36. Keller J.U., Gobel M.U., The thermo-valve: a device for expanding compressed liquids and simultaneously gaining heat, *KI, Luft- und Kältetechnik*, (1997), Vol. 33 (2), pp. 57-60.
37. Poshernev N.V., Khodorkov I.L., "Experience from the operation of a conical vortex tube with natural gas", *Chem. Pet. Eng.*, (2003), Vol. 37 (9-10), pp. 602-607.
38. Cao Y., Liu J., Gong M. Luo E, Wu J., Chen G., "An experimental research on the performance of a small flow vortex tube", *J. Eng. Therm.*, (2005), Vol. 1, pp. 14-17.
39. Dincer K., Baskaya S., Kirmaci V., "Investigation of performance of a vortex tube with air, oxygen, carbon dioxide and nitrogen as working fluids", *Energy*, (2006), Vol. 47, pp. 36-40.
40. Aydin O., Baki M., "An experimental study on the design parameters of a counter flow vortex tube", *Energy*, (2006), Vol. 31 (14), pp. 2763-2772.
41. Jeffery M., Gordon and Ahlborn Boye K., "The vortex tube as a classical thermodynamics refrigeration cycle", *AIP Journal of Physics*, (2012), Vol. 11, 024312.

42. Williams D.T., "Ranque-Hilsch Vortex Tube for Refrigeration in Developing Communities", In. *dissigno*, San Francisco, CA USA, (2005), Vol.30, pp. 1-5.
43. Stanescu G., Errera M.R., Rocha L.A.O., "Energy recovering during gas pressure letdown process in natural gas pipeline transmission", *Proceedings of the 20th International Congress of Mechanical Engineering*, Gramado-RS, Brazil, (2009).
44. Stanescu G., Rocha, L. A. O., Costa J.A.V., Vargas, J.V.C., "Study of a Vortex —tube equipped column reactor for solid state fermentation", *Proceedings of the 7th Brazilian Congress of Engineering and Thermal Sciences*, Rio de Janeiro, RJ, Brazil, (1998), Vol. 1.
45. Amitani T., Adachi T., and Kato T., "A study on temperature separation in a large vortex tube", *Jnrm. Soc. Mech. Eng.*, (1983), Vol. 49, pp. 877-884.
46. Lindstrom Lang C.U., "The three dimensional distribution of tangential velocity and total temperature in vortex tubes" *J. Fluid. Mech.*, (1971), Vol. 45, pp. 161-187.
47. Westley R., "Vortex Tube Performance Data Sheets", *College of Aeronautics, Canfield*, (1967).
48. R. Shamsoddini, A.H. Nezhad, Numerical analysis of the effects of nozzles number on the flow and power of cooling of a vortex tube, *Int. J. Refrig.* , (2010), Vol. 33, pp. 774-782.
49. Liew R., Michalek W.R., Zeegers J.C.H., and Kuerten J.G.M., "droplet behavior in vortex tube", *Journal of Physics: Conference Series*, (2011), Vol. 5, pp. 318-323.
50. Sazhin, S. S., Abdelghaffar, W. A., Krutitskii, P. A., Sazhina, E. M. & Heikal, M. R., "New approaches to numerical modelling of droplet transient heating and evaporation", *Int. Journal of Heat and Mass Transfer*, (2005), Vol. 48, pp. 4215–4228.
51. Guillaume D.W., Jolly Lii J.L., "Demonstrating the achievement of lower temperature with two-stage vortex tubes", *review of scientific instruments*, (2001), Vol. 72, pp. 3346-3348.
52. Eiamsa-ard S.A., Wongcharee K., Promvongse P., "Experimental investigation on energy separation in a counter flow RH vortex tube, Effect of cooling a hot tube", *ICHMT*, (2010), vol. 56, pp. 162.
53. Takahama H., Kawamura H., Kato S., Yokosava H., "Performances characteristics of energy separation in steam operated vortex tube", *International journal of science*, (1979), Vol. 14, pp. 735-744.
54. Takahama V., "Studies on vortex tube"; *Bull. JSME*, (1965), Vol. 8, pp. 433-440.

55. Takahama H., Yokosava H., Ohara T., "Study on vortex tube (use divergent tube to shorten length of main chamber)", *Trans. Japan soc. Mech. Engrs. SER.B*, (1980), Vol. 46, pp. 584-592.
56. Soni Y., "Parametric study of Ranque Hilsch vortex tube", university of Idaho, (1973).
57. Arbutov V.A., Yu, Dubnischchev N., Lebedev A.V., Kh. Pravdina M., and Yavorski N. I., "Observation of large-scale hydrodynamic structures in a vortex tube and the Ranque effect", *American institute of physics*, (1997), Vol. 23, pp. 84-90.
58. Hamoudi A. F., Fartaj A., Rankin G. W., "Performance Characteristics of a Micro scale Ranque–Hilsch Vortex Tube", *Journal of Fluid Mechanics*, 2008, Vol. 130.
59. Mohammad S. V., Nima N., "Experimental modeling of a curved Ranque-Hilsch vortex tube refrigerator", *International Journal of Refrigeration*, 2011, Vol. 34, pp. 1109-1116.
60. Agrawal N., Naik S.S, Gawale Y.P., "Experimental investigation of vortex tube using natural substances", *International Communications in Heat and Mass Transfer*, 2014, Vol. 52, pp. 51-52.
61. Duspara M., Kosec B., Stoic M., Kramar D., Stoic A., "Application of Vortex Tube for Tool Cooling", *Journal of Production Engineering*, 2013, Vol. 16.
62. Jose Roberto S.M., "An air-standard cycle and a thermodynamic perspective on operational limits of Ranque–Hilsch or vortex tubes", *International Journal of Refrigeration*, 2010, Vol. 33, pp.765-773.
63. Sudhakar Subudhi and Mihir Sen, "Review of Ranque–Hilsch vortex tube experiments using air", *Renewable and Sustainable Energy Reviews*, 2015, Vol. 52, pp.172-178.